Journal of Marine Research, 59, 859–894, 2001

A data assimilative marine ecosystem model of the central equatorial Pacific: Numerical twin experiments

by Marjorie A. M. Friedrichs[1]

ABSTRACT

A five-component, data assimilative marine ecosystem model is developed for the high-nutrient low-chlorophyll region of the central equatorial Pacific (0N, 140W). Identical twin experiments, in which model-generated synthetic 'data' are assimilated into the model, are employed to determine the feasibility of improving simulation skill by assimilating *in situ* cruise data (plankton, nutrients and primary production) and remotely-sensed ocean color data. Simple data assimilative schemes such as data insertion or nudging may be insufficient for lower trophic level marine ecosystem models, since they require long time-series of daily to weekly plankton and nutrient data as well as adequate knowledge of the governing ecosystem parameters. In contrast, the variational adjoint technique, which minimizes model-data misfits by optimizing tunable ecosystem parameters, holds much promise for assimilating biological data into marine ecosystem models. Using sampling strategies typical of those employed during the U.S. Joint Global Flux Study (JGOFS) equatorial Pacific process study and the remotely-sensed ocean color data available from the Sea-viewing Wide Field-of-view Sensor (SeaWiFS), parameters that characterize processes such as growth, grazing, mortality, and recycling can be estimated. Simulation skill is improved even if synthetic data associated with 40% random noise are assimilated; however, the presence of biases of 10–20% proves to be more detrimental to the assimilation results. Although increasing the length of the assimilated time series improves simulation skill if random errors are present in the data, simulation skill may deteriorate as more biased data are assimilated. As biological data sets, including *in situ,* satellite and acoustic sources, continue to grow, data assimilative biological-physical models will play an increasingly crucial role in large interdisciplinary oceanographic observational programs.

1. Introduction

Methods for systematically constraining dynamical models with available data extend back to engineering control theory and geophysics; however, the terminology "data assimilation" itself was developed in meteorology in the 1960s and was originally used to describe the technique(s) of using observations to improve the forecasting skill of operational models (Malanotte-Rizzoli and Tziperman, 1996). In the following decade, physical oceanographic data assimilative models began to be developed; however the lack

1. Center for Coastal Physical Oceanography, Crittenton Hall, Old Dominion University, Norfolk, Virginia, 23529, U.S.A. ***email: marjy@ccpo.odu.edu***

of a unifying objective for oceanographic data assimilation, such as the driving force of numerical weather prediction for meteorology, caused oceanographers to define data assimilation much more broadly (Malanotte-Rizzoli and Tziperman, 1996). In physical oceanography, data assimilation refers to many different techniques of combining dynamical models with observations, and is not only used for ocean forecast (Peloquin, 1992; De Maria and Jones, 1993; Carnes *et al.,* 1996; Aikman *et al.,* 1996), but is also often used to quantitatively and systematically test and improve poorly known subgrid-scale parameterizations and boundary conditions that are abundant in many numerical models (Seiler, 1993; Lardner and Das, 1994; Gunson and Malanotte-Rizzoli, 1996a; Ullman and Wilson, 1998).

Just as the scientific community witnessed the evolution of a new generation of data assimilative physical oceanographic models in the 1970s and 1980s, in the past several years the field of data assimilative biogeochemical ocean modeling has begun to emerge; however, just as the many innate differences between meteorology and physical oceanography have caused data assimilation goals and techniques to evolve very differently in these two fields, differences between physical and biological oceanography are also resulting in substantial differences between these types of data assimilation (Hofmann and Friedrichs, 2001a). Because biological systems have no analog to the fluid dynamicists' Navier-Stokes equations, ecosystem models are by necessity empirical, nonlinear, and abound with poorly known formulations. Such models typically include large numbers of parameters that are difficult, or even impossible to measure with current oceanographic instrumentation. As a result, data assimilation methods are often applied to marine ecosystem models in order to test different parameterizations of biogeochemical processes (Matear, 1995) and to estimate optimal parameter values (Evans, 1999; Vallino, 2000). Space and time scales in physical and biological oceanographic systems can also be different. The rapid doubling rates of the most abundant phytoplankton species $O(1\ d^{-1})$ may cause the synoptic time scales of these systems to resemble their meteorological counterparts (O(days)) as opposed to the physical oceanographic scales of several months. Furthermore, just as there are much less physical oceanographic data than meteorological data, there may be equally less biological data than physical data.

For these reasons, the application of data assimilation techniques to biogeochemical ocean models, and specifically to marine ecosystem models, presents many exciting new challenges (Hofmann and Friedrichs, 2001a). In the past decade large interdisciplinary programs, e.g. the Joint Global Ocean Flux Study (JGOFS), have included model prediction and forecast as specific research objectives (Sarmiento *et al.,* 1987; Abbott, 1992). However, new studies are revealing that much more work needs to be performed before this becomes a realistic and achievable goal (Sarmiento and Armstrong, 1997). It is rapidly becoming evident that until high resolution biological and chemical data are available over large regions of the ocean, and until a much clearer understanding of the intricacies of marine ecosystems is attained, data assimilation in ecosystem models will be more useful for model improvement and parameter estimation (Matear, 1995; Fasham and

Evans, 1995; Prunet *et al.,* 1996a,b; McGillicuddy *et al.,* 1998; Spitz *et al.,* 1998; Evans, 1999; Hurtt and Armstrong, 1999; Vallino, 2000) rather than model prediction and forecast (Hofmann and Friedrichs, 2001b).

Many methods for combining model dynamics with data exist. One particularly straightforward method entails replacing the model solution with data whenever such information is available. This technique, referred to as data insertion, integrates the model forward in time until additional observations become available, at which point the model is reinitialized, and the process repeated. In an initial application of data insertion in physical oceanography, Holland and Hirschman (1972) attempted to estimate velocity fields by inserting temperature and salinity data into relatively complex ocean models. Model-data inconsistencies caused the resulting simulations to compare poorly with observations. This led to the development of techniques in which the model solution is nudged toward observations, instead of being replaced by observations, whenever data become available. Although this method represents a significant improvement over the earlier insertion technique, it still lacks a means by which information on data uncertainty can be incorporated, and does not provide an estimate of the uncertainties of the resulting solution (Sarmiento and Bryan, 1982; Holland and Malanotte-Rizzoli, 1989; Malanotte-Rizzoli and Young, 1995). Data insertion and nudging have also been applied to simple marine ecosystem models (Ishizaka, 1990; Armstrong *et al.,* 1995). In these studies, chlorophyll estimates made from satellite ocean color measurements were the only biological data available for assimilation. Although estimates of phytoplankton biomass were improved as a result of the assimilation, the accuracy of other model components was reduced. Nudging has also been used to keep an ecosystem model from drifting (Moisan and Hofmann, 1996) or to represent unresolved biological processes (Najjar *et al.,* 1992).

More sophisticated assimilation schemes such as optimal interpolation and the Kalman filter have been successfully applied to weather forecast models by meteorologists, yet hold little hope for marine ecosystem models because of the inherent nonlinearities of biological systems. Instead, schemes which have recently been applied to nonlinear physical oceanographic systems, such as the variational adjoint method (Tziperman and Thacker, 1989), the Extended Kalman Filter (Evensen, 1992), and simulated annealing (Barth and Wunsch, 1990; Kruger, 1993), may be more applicable to biological problems. These methods can be used to determine an optimal solution that maximizes agreement between the model solution and the observations. Both the variational adjoint method and simulated annealing have been successfully used to assimilate biological data into marine ecosystem models (Matear, 1995; Hurtt and Armstrong, 1996, 1999; McGillicuddy *et al.,* 1998; Friedrichs, 2001), and have their respective advantages and drawbacks. The variational adjoint method can be used to efficiently estimate best-fit values for unknown model parameters and rate coefficients; however, because of the nonlinear nature of marine ecosystem models, it is possible that an adjoint method may lead to multiple suboptimal parameter sets, thereby necessitating techniques for identifying a single optimal set of parameters. The stochastic, 'random-walk' nature of simulated annealing may allow the

investigation of more parameter values resulting in a greater ability to identify the global optimum parameter set, but this technique is less efficient than the adjoint method. Both simulated annealing and the Extended Kalman Filter may be computationally too intensive to be of wide-scale use in large-scale biological oceanographic assimilation analyses.

Before the application of these types of data assimilation techniques to marine ecosystem models becomes routine, a number of methodological issues need to be addressed. For example, it is not yet clear under what conditions different assimilation schemes will be most appropriate, what sampling strategies will be optimal, or what levels of imprecision or inaccuracies in the measurements will be acceptable. One method for addressing such methodological issues is through the use of numerical twin experiments, in which model-generated data are assimilated into a model. Although the utility of numerical twin experiments is well accepted within the fields of meteorology and physical oceanography (Ghil and Malanotte-Rizzoli, 1991; Sheinbaum, 1995; Gunson and Malanotte-Rizzoli, 1996a,b), this approach has only recently been applied to ecosystem modeling analyses. Lawson *et al.* (1995; 1996) first used these types of experiments to demonstrate the feasibility of applying the adjoint method to recover optimal values for various ecosystem parameters. They determined that the assimilation of data at monthly intervals was adequate for the recovery of most rate parameters. Although bi-weekly data collection significantly enhanced the results, weekly assimilation provided no further improvement. Harmon and Challenor (1997) used numerical experiments to assess the success of a new Monte Carlo Markov Chain data assimilation algorithm specifically developed for use with highly nonlinear ecosystem models. Twin experiments have also been used to determine if model parameters can be estimated independently, and thus whether or not a given model will need to be simplified (Spitz *et al.,* 1998). Even more recently, Gunson *et al.* (1999) seeded numerical floats in an eddy-permitting basin-scale model of the North Atlantic Ocean, and followed their trajectories with a one-dimensional biological model. Using twin experiments to assimilate simulated ocean color data, the authors were able to determine which parameters could be recovered in different regions of the model domain.

In this paper, the ecosystem model described by Friedrichs and Hofmann (2001; hereafter referred to as FH01) is run in a data assimilative mode. In the following section, methodological details of the ecosystem model, the adjoint method, and the numerical twin experiments are presented. Twin experiments are then conducted in order to (i) compare the results of simple and sophisticated assimilation schemes, (ii) determine the effects of assimilating biological data that contain random errors and biases, and (iii) assess both the suitability of assimilating *in situ* cruise data versus remotely-sensed ocean color data as well as the effects of varying sampling strategy and frequency of data collection (Section 3). The paper concludes with a discussion and summary section (Section 4) as well as a section describing some future challenges for data assimilative marine ecosystem modeling (Section 5).

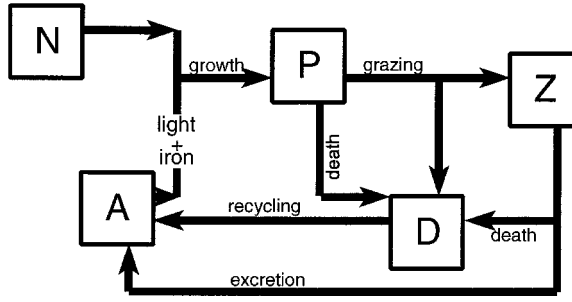

Figure 1. Schematic of the five-component ecosystem model: phytoplankton (P), zooplankton (Z), ammonium (A), nitrate (N) and detritus (D). Adapted from Friedrichs and Hofmann (2001).

2. Methods

a. Ecosystem model

The ecosystem model of FH01 contains five model components (phytoplankton (P), zooplankton (Z), ammonium (A), nitrate (N), and detritus (D); Fig. 1) and has been developed for use in the central equatorial Pacific (i.e. 0N, 140W). Because of the rapid growth rates of the picoplankton and microzooplankton in this region ($O(1\ \mathrm{d}^{-1})$), the biology directly responds to physical forcing on relatively short (daily) time scales. As a result, the model is not forced by ocean general circulation model output as is typical for one-dimensional marine ecosystem models (Fasham *et al.,* 1993; Leonard *et al.,* 1999; McClain *et al.,* 1999; Gunson *et al.,* 1999), rather it is forced using daily observations of solar radiation, temperature (T), and velocity (u, v) obtained from the extensive Tropical-Atmosphere Ocean (TAO) mooring array (McPhaden *et al.,* 1998). Daily vertical profiles of vertical velocity ($w(z)$) are also computed from TAO data (u, v, and T) according to the method of FH01. Based on recent observations from the equatorial Pacific, iron limitation of the phytoplankton is assumed *a priori* (Frost, 1996; Behrenfeld *et al.,* 1996). Daily vertical profiles of iron concentration are derived from the empirical formulation of Gordon *et al.* (1997) combined with a deep $Fe{:}T$ relationship (Friedrichs, 1999; FH01). A brief outline of the model equations is included in the Appendix and a more thorough discussion of the model formulations is given in FH01. Based on a review of the literature describing the biology of the equatorial Pacific, best estimates of the model parameters are made (Table 1). Model runs begin on September 1, 1991 (Fig. 2).

b. Variational adjoint implementation

In this study, both the relatively straightforward technique of data insertion as well as the more sophisticated adjoint method are applied to the FH01 ecosystem model. We provide a brief overview of how the variational adjoint method is specifically applied to the FH01 ecosystem model. Detailed descriptions of the variational adjoint method appear in Wunsch (1996) and Bennett (1992).

Table 1. Values, units, and definitions of the parameters used in the biological model.

Parameter	Value	Units	Definition
w_Z	0.5	m d^{-1}	Z sinking rate
w_D	12	m d^{-1}	D sinking rate
φ_P	0.45	d^{-1}	P loss rate
φ_Z	0.75	d^{-1}	Z loss rate
γ	0.75	(none)	Z assimilation efficiency
β	0.3	(none)	A regeneration fraction
r_D	1	d^{-1}	D regeneration rate
g	29	d^{-1}	Z maximum grazing rate
Λ	1	(mmol N m^{-3})$^{-1}$	Ivlev grazing parameter
k_{Fe}	0.034	μmol Fe m^{-3}	Iron half-saturation value
α	29	d^{-1} (E m^{-2} h^{-1})$^{-1}$	Initial slope of P-I curve
P_M	14	d^{-1}	Max. rate of photosynthesis
k_A	0.1	mmol N m^{-3}	A half-saturation value
d_c	45	m	Depth of max. P, A conc.
Fe_{min}	0.026	μmol Fe m^{-3}	Min. concentration of iron
m_{Fe}	0.001	μmol Fe m^{-4}	Slope of iron profile

i. Cost function. The FH01 ecosystem model is run forward in time using the parameter values listed in Table 1, in order to obtain a value of the cost function, which is defined to be a measure of the misfit between the predicted variables (a) and observed variables ($\hat{a}$). Assuming that the errors in the data set to be assimilated are uncorrelated, the general cost function, J, can be mathematically expressed as a weighted sum of squares:

$$J = \frac{1}{2} \sum_{i=1}^{M} \sum_{j=1}^{N} w_i (a_{ij} - \hat{a}_{ij})^2. \tag{1}$$

The sums are carried out over the number of time-steps (N days) as well as the number of variables ($M = 5$) for which observations are available: P, Z, A, N, and the rate of primary production (PP). The weights, w_i, account for differences in the relative magnitudes of the ecosystem components. For example, if data are not available then $w_i = 0$. If data are available, then $w_i = \max_i (\langle a_i \rangle)/\langle a_i \rangle$, where $\langle a_i \rangle$ is the time average of a_i over the entire two-year model simulation, and $\max_i (\langle a_i \rangle)$ is the maximum value of these five time-averages ($\langle PP \rangle$, $\langle P \rangle$, $\langle Z \rangle$, $\langle A \rangle$, $\langle N \rangle$) (Lawson *et al.,* 1996). Numerical twin experiments are used *a posteriori* to test the sensitivity of the assimilation results to this particular choice of weights. On average, doubling or halving any single value of w_i changed the errors in the resulting parameter estimates by less than 3%. Although it is possible to include separate terms in the definition of the cost function in order to allow *a priori* constraints or penalties on the parameter values (McGillicuddy *et al.,* 1998; Gunson *et al.,* 1999), because of the high degree of uncertainty associated with the values of many of the ecosystem parameters, and in order to maintain the highest possible degree of freedom in the model control variables, no upper or lower limits are imposed on any of the parameter values.

An adjoint, or backward model, is used to compute the gradients of the cost function

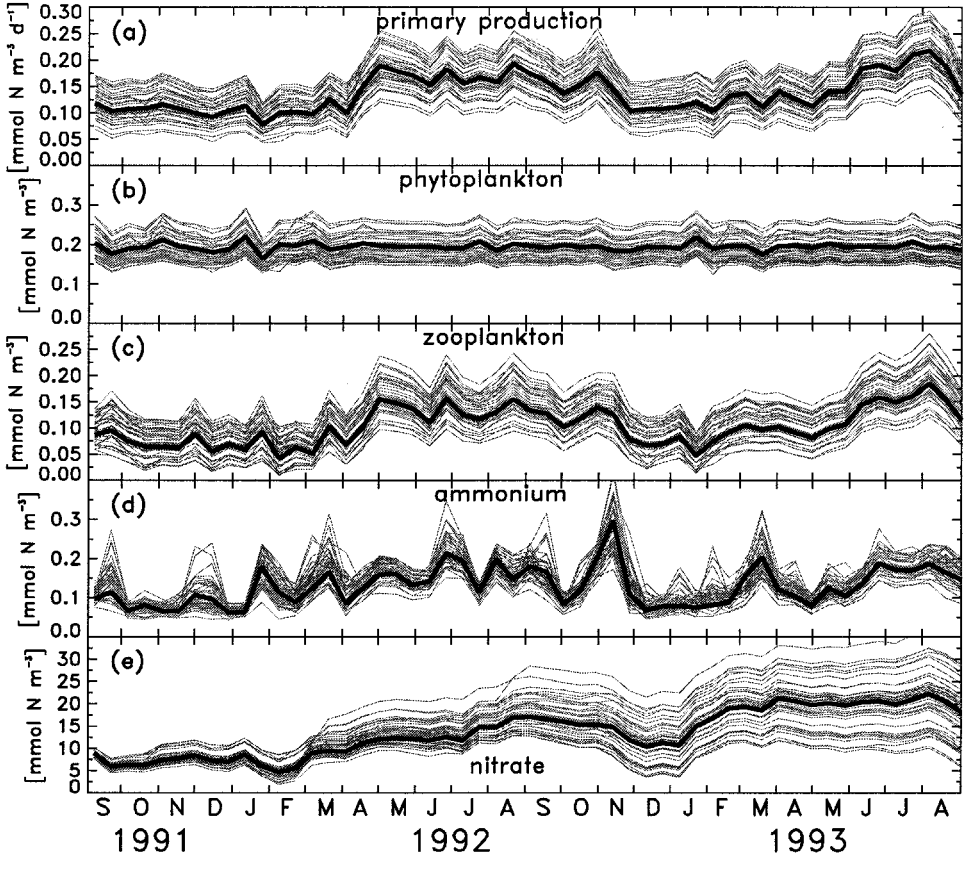

Figure 2. Fifty simulated time series (thin lines) of (a) $\rho_{PP}(t)$, (b) $\rho_P(t)$, (c) $\rho_Z(t)$, (d) $\rho_A(t)$, and (e) $\rho_N(t)$ averaged over fourteen days and generated using imperfect random values for the model control variables which fall within the *a priori* uncertainty ranges of Table 3. The true simulation (heavy lines; $\hat{C}(t)$) is generated using values of 1.0 for all six scaled control variables. All simulations represent vertical averages over the euphotic zone.

with respect to the input parameter set, frequently referred to as the set of 'model control variables.' The technique developed by Lawson *et al.* (1995) is used to construct the adjoint code directly from the model code by means of Lagrange multipliers. Values of these gradients are passed to a variable-storage quasi-Newton optimization procedure (Gilbert and Lemarechal, 1989) which computes the optimal direction toward the minimum of the cost function, and the optimal step size in that direction. New values of the control variables that yield a smaller misfit between the model solution and observations are then used to rerun the model, and recompute the cost function. The process of running the adjoint model and the optimization routine continues iteratively until the control variables converge to values which maximize agreement between the model-derived

quantities and the observations; i.e., until the minimum of the cost function is identified. Uncertainties in the recovered values of the control variables are computed from a finite difference approximation of the Hessian matrix of the cost function at its minimum (Tziperman and Thacker, 1989; Matear, 1995; Gunson and Malanotte-Rizzoli, 1996b).

ii. Model control variables. Model control variables can consist of a variety of unknowns, such as component initial conditions, empirical model coefficients, and parameters related to model forcing. Because ecosystem model components (e.g., plankton concentrations) typically become independent of their initial values quite quickly, it is often not necessary nor feasible to use the adjoint method to estimate component initial conditions (Friedrichs, 1999). Conversely, the numerous poorly known model parameters which characterize many ecosystem models may constitute appropriate choices for the control variables; however, the inherent nonlinearities associated with most ecosystem models frequently cause many model parameters to be highly correlated (Matear, 1995). If correlated parameters are chosen as control variables in an adjoint analysis, the system may become underdetermined resulting in large uncertainties in the estimated parameter values. An alternative approach consists of choosing the control variables to be the subset of model parameters which are uncorrelated, or at most weakly correlated (Friedrichs, 1999, 2001).

Although formal methods exist for determining the degree of correlation between pairs of model parameters (Matear, 1995), in this study the results of a sensitivity analysis are used to estimate the degree of correlation between various model parameters. The sensitivity of a certain model component or model diagnostic (C) to a given model parameter (k) can be quantified by calculating the normalized sensitivity ($S_{C,k}$) defined as the fractional change in C due to a fractional (25%) increase in the value of k (FH01):

$$S_{C,k} = \frac{\dfrac{C_R - C_S}{C_S}}{\dfrac{k_R - k_S}{k_S}}. \tag{2}$$

In this notation, C_R is the steady-state value of P, Z, A, N, or PP obtained using the reference parameter value (k_R; Table 1), whereas C_S is the analogous value obtained using $k_S = 1.25k_R$. (Note that $S_{C,k}$ is a good measure of sensitivity only as long as C does not have maxima or minima over the interval k_R to k_S. Experiments using other fractional increases (10%, 20%) indicate that this is the case for nearly all the parameter values listed in Table 2.)

Similarities in the absolute magnitudes of S_P, S_Z, S_A, S_N, and S_{PP} (Table 2) for φ_Z and γ suggest that these parameters are highly correlated. Similarly, the S_C for Λ are about twice that of g, indicating that these two parameters are also correlated. These two pairs of zooplankton-related parameters are distinct from the iron-related parameters which also appear to be highly correlated: k_{Fe}, Fe_{min}, and m_{Fe}. Two other correlated parameter

Table 2. Results of model sensitivity analysis. Sensitivities (S_C) to parameters are computed according to Eq. (2). Dashes indicate model insensitivity ($|S_c| < 0.15$) to parameter changes.

Parameter	S_P	S_Z	S_A	S_N	S_{PP}
g	−0.4	−0.3	—	−0.3	−0.4
Λ	−0.8	−0.5	0.2	−0.5	−0.7
φ_Z	0.5	−0.6	—	0.3	0.4
γ	−0.4	0.7	—	−0.3	−0.4
k_{Fe}	—	−0.9	−0.7	—	−0.5
Fe_{min}	—	0.7	0.6	—	0.3
m_{Fe}	—	−0.3	−0.2	—	—
P_M	—	1.0	—	—	0.5
α	—	0.8	—	—	0.4
d_c	—	−0.6	—	—	−0.3
φ_P	—	−1.0	—	—	—
k_A	—	—	1.0	—	—
r_D	—	—	0.2	—	—
w_D	—	—	−0.2	—	—
w_Z	—	—	—	—	—
β	—	—	—	—	—

triplets include P_M, α, and d_c, as well as k_A, r_D, and w_D. Parameter φ_P is relatively independent of the other model parameters.

Based on this sensitivity analysis, the set of model control variables is chosen to include φ_P, as well as one parameter from each of the five correlated parameter pairs/triplets discussed above: φ_P, P_M, k_{Fe}, φ_Z, g and r_D. The specific parameter choice (from the two or three included in the pair/triplet) is generally based on the sensitivity of the cost function to each parameter. Since the value of k_{Fe} typically affects the value of the cost function much more than either Fe_{min} or m_{Fe}, the set of control variables includes k_{Fe}.

An *a posteriori* error analysis indicates that the assimilation results are not sensitive to the specific choice of these six parameters. For example, similar results are obtained if the model control variables P_M and r_D are replaced with α and k_A, respectively. Similarly, the mean error associated with the set of six recovered control variables is independent of whether the Ivlev grazing parameter (Λ) or the maximum grazing rate (g) is chosen as a model control variable; however, if both Λ and g are included as control variables, the mean error in the (seven) model control variables increases by more than an order of magnitude. As discussed above, it is the correlation of Λ and g that causes this increased error. Only independent model parameters can be successfully recovered in a least-squares type of analysis.

Values of the control variables vary over many orders of magnitude (Table 3). To avoid precision problems with the data assimilative model, these values are scaled to give the control variables more uniform magnitudes. The control variables are non-dimensionalized as: $P_M = c_1 P'_M$, $\varphi_Z = c_2 \varphi'_Z$, $k_{Fe} = c_3 k'_{Fe}$, $\varphi_P = c_4 \varphi'_P$, $g = c_5 g'$, $r_D = c_6 r'_D$, where c_i are constant scaling factors (Table 3). Scaled control variables with values of 1.0 represent the best estimates available from experimental studies; however, these best estimates are associated with relatively high levels of uncertainty. To obtain growth and grazing rates in

Table 3. Scaled control variables and scaling factors.

Scaled control variable	*A priori* range of values for scaled control variables	Scaling factor	Value of scaling factor
P'_M	1.0 ± 0.3	c_1	$14\ d^{-1}$
φ'_Z	1.0 ± 0.3	c_2	$0.75\ d^{-1}$
k'_{Fe}	1.0 ± 0.3	c_3	$0.034\ \mu mol\ Fe\ m^{-3}$
φ'_P	1.0 ± 0.3	c_4	$0.45\ d^{-1}$
g'	1.0 ± 0.5	c_5	$29\ d^{-1}$
r'_D	1.0 ± 0.5	c_6	$1.0\ d^{-1}$

agreement with those of Landry *et al.* (1995) and Verity *et al.* (1996) (Table 6 of FH01), values of P'_M and k'_{Fe} could be anywhere within the range 1.0 ± 0.3, and that of g' could be within the range 1.0 ± 0.5 (Table 3). Similarly, non-negative nitrate concentrations and *f*-ratios in agreement with those of McCarthy *et al.* (1996) are obtained if r'_D is in the range 1.0 ± 0.5. Estimates of φ'_P and φ'_Z are nearly nonexistent, yet the model is quite sensitive to choices for these parameters; e.g., the model fails if the value of φ'_Z exceeds 1.3. As discussed in more detail below, these uncertainty ranges (Table 3) are used to randomly select *a priori* values for the model control variables.

There is no guarantee that the adjoint method will always identify the global minimum of the cost function; it is possible that different relative minima may be identified, depending on the initial *a priori* values assigned to the model control variables. Therefore, in order to test the sensitivity of the assimilation results to the specific *a priori* values initially assigned to the model control variables, a uniform random number generator is used to select fifty distinct *a priori* estimates for each of the six model control variables such that they are constrained to fall within the uncertainty ranges of Table 3. If the same set of optimal parameter values is returned in each of the fifty assimilation runs, it is highly likely that the global minimum of the cost function has been located.

c. Numerical twin experiments

In a numerical twin experiment, a model is initially run in order to provide a "true" simulated time series ($\hat{C}(t)$), which is subsampled in order to create a model-generated synthetic data set. The model is then run a second time using an imperfect set of model control variables, to generate a "reference" (no assimilation) time series ($\rho_c(t)$). This same imperfect parameter set is used in the third and final model run, but this time the synthetic data are assimilated into the model in order to generate a new time series ($C(t)$). The success of the twin experiment is judged by the degree of agreement between these results and the true simulation.

In this analysis, numerical twin experiments are performed (i) to compare results obtained using data insertion with those obtained via the adjoint method, (ii) to determine the impact of assimilating data containing known levels of random noise and biases, and (iii) to examine whether the sampling strategies of the U.S. JGOFS EqPac experiment

Table 4. Descriptions of data sets used in numerical twin experiments.

Data set	Cruise data	Satellite data
DSI	*PP*, *P*, *Z*, *A*, *N* every other day for 20 days starting on YD276*	none
DSII	none	*P* every other day for six months starting on YD1
DSIII	*PP*, *P*, *Z*, *A*, *N* on YD87 and YD89	*P* every other day for six months starting on YD1

*The notation YD276 refers to the 276th day of 1992.

(Murray *et al.,* 1994, 1995) and the remotely-sensed ocean color data available from the Sea-viewing Wide Field-of-view Sensor (SeaWiFS) (McClain *et al.,* 1998) are adequate for parameter estimation studies.

To accomplish these goals, three synthetic data sets, subsampled using different sampling strategies, are assimilated. Data Set I (DSI; Table 4) is obtained by subsampling the true simulation using a sampling strategy characteristic of the JGOFS EqPac Time Series II cruise: *PP*, *P*, *Z*, *A*, and *N* are sampled every other day for 20 days beginning on YD276. Data Set II (DSII) is obtained by subsampling the true *P* simulation every other day for 6 months beginning on YD1, and is typical of the data available from SeaWiFS. As a result of cloud cover and satellite path, ocean color data within a 10° longitude and 2° latitude region centered on 0N, 140W, are typically available 50% of the time. Data Set III combines Data Set II with *PP*, *P*, *Z*, *A*, and *N* cruise data from two days in 1992.

Because biological and chemical measurements may contain large uncertainties, it is crucial to quantify the effect of assimilating model-generated data with known levels of noise. As a first approximation, instrument imprecision is accounted for by adding various levels of uniform random noise to the synthetic data sets. For example, a time series with 20% random noise is created by randomly generating a time series of numbers within the range $[-0.2, 0.2]$, multiplying this by the original (true) time series, and adding the resulting time series to the original time series. A data set associated with 20% random noise thus represents data to which a *maximum* of 20% noise has been added. The deleterious effects of assimilating biased data are also investigated. A data set with 20% bias is created by multiplying the true simulated time series by a constant factor of 1.2.

To quantify the success of a particular numerical experiment, two measures of misfit are calculated. First, the variable R_c is introduced to quantify the original disagreement that exists prior to the assimilation process; i.e., the misfit between the true simulation of component C computed using values of 1.0 for each of the scaled model control variables ($\hat{C}(t)$), and the reference simulation generated using a randomly selected (from the *a priori* ranges of values listed in Table 3) imperfect set of control variables ($\rho_c(t)$):

$$R_c(t) = \frac{|\hat{C}(t) - \rho_c(t)|}{\hat{C}(t)}. \tag{3}$$

Time-averaged (over the 730 day model run) values of this *a priori* misfit are defined: $\langle R_c \rangle = \langle |\hat{C}(t) - \rho_c(t)| \rangle / \langle \hat{C} \rangle$. Because $\langle \hat{C} \rangle$ is always nonzero, this particular definition ensures that $\langle \overline{R_c} \rangle$ remains finite. The mean *a priori* misfits for the fifty reference simulations are: $\langle \overline{R_{PP}} \rangle = 0.15$, $\langle \overline{R_P} \rangle = 0.15$, $\langle \overline{R_Z} \rangle = 0.27$, $\langle \overline{R_A} \rangle = 0.25$, and $\langle \overline{R_N} \rangle = 0.20$.

A second measure of misfit, $\Psi_c(t)$, is defined as the misfit that remains *after* the assimilation experiment is complete, i.e. the misfit between the true simulation ($\hat{C}(t)$) and the simulated time series obtained from an assimilation experiment ($C(t)$):

$$\Psi_c(t) = \frac{|\hat{C}(t) - C(t)|}{\hat{C}(t)}. \tag{4}$$

The time-averaged value of the post-assimilation misfit is defined: $\langle \Psi_c \rangle = \langle |\hat{C} - C| \rangle / \langle \hat{C} \rangle$. Note that although $\Psi_c(t)$ may approach infinity if $\hat{C}(t)$ approaches zero, $\langle \Psi_c \rangle$ remains finite since $\langle \hat{C} \rangle$ is always nonzero.

d. Reference simulations ($\rho_c(t)$)

Fifty reference simulations for phytoplankton ($\rho_P(t)$), zooplankton ($\rho_Z(t)$), ammonium ($\rho_A(t)$), nitrate ($\rho_N(t)$) and primary production ($\rho_{PP}(t)$) (Fig. 2) are generated using fifty distinct sets of *a priori* parameter estimates (randomly chosen such that they are constrained to fall within the uncertainty ranges of Table 3). These simulations illustrate how large differences in plankton and nutrient concentrations can result from relatively small changes in parameter values. Even if relatively conservative estimates of parameter uncertainties are made (Table 3), model components can often not be constrained to within a factor of 5 or more. For example, nitrate concentration at the end of 1993 could range anywhere from 5 mmol N m^{-3} to 40 mmol N m^{-3} (Fig. 2), depending on the various reasonable choices made for the model parameters. Although generally the fifty reference simulations are within $\pm$30–50% of the true simulation, during the time periods when zooplankton and ammonium reach particularly low concentrations, zooplankton and ammonium can differ from those of the true simulation by more than 100%.

The characteristics of the nitrate simulations are very different from those of PP, P, Z, and A: whereas the envelopes for the plankton and ammonium simulations appear to remain tight and nearly constant in time, the envelope of the 50 nitrate simulations broadens over time. This is because plankton and ammonium concentrations are dominated by biological processes which have very short $O(1\ d^{-1})$ time scales, and are characterized by a quick (2–5 day) loss of memory of the initial conditions. Because the Figure 2 time series are averaged over a time period (two weeks) which exceeds the time period of this memory loss (several days), it appears that these model components instantaneously become independent of their initial conditions, even though in actuality this occurs over a time span of several days. Thus, the width of the envelope of the 50 PP, P, Z, and A simulations is not governed by initial conditions, but rather is a function of the ranges of parameter values used for the fifty simulations. On the contrary, nitrate concentration is primarily determined by physical advective processes which have much longer time scales.

As a result, nitrate remains dependent on initial conditions throughout the entire two-year simulation, causing the envelope of 50 simulations to gradually expand through time.

3. Results

a. Comparison of assimilation schemes

i. Data insertion. Data insertion experiments are performed in which Data Sets I and II (Table 4) are inserted into the ecosystem model. The insertion of Data Set I (synthetic cruise data) results in time series of $\Psi_c(t)$ which are identical to those of $R_c(t)$ until the day on which the first data are inserted on YD276 (Fig. 3). On this date, and on the other nine days when data are inserted, $\Psi_c(t)$ drops to zero as expected; however, on alternate days when data are unavailable (YD277, YD279...) values of Ψ_c are large. Because the synthetic data are derived using parameter values that may be quite different from those used to run the model, the insertion of data may cause instabilities in the model. As a result, it is possible for values of Ψ_c computed after the insertion of DSI (e.g. Ψ_P and Ψ_A on YD277, YD279) to exceed the corresponding values of R_c computed without data assimilation.

After all available data have been inserted, values of Ψ_{PP}, Ψ_P, Ψ_Z and Ψ_A overshoot the corresponding *a priori* time series (R_c), indicating that as soon as data are no longer available, a deterioration in simulation skill quickly results. Only 5–10 days after the insertion is complete, the assimilation time series converge to the corresponding reference (no assimilation) time series. This rapid convergence is due to the insensitivity of the model to the component initial conditions, which in turn results from the short (O(1 day)) time scales of the dominant biological processes (e.g. growth, grazing). Thus, the success of assimilation schemes such as data insertion and nudging will depend on time series observations of nutrient concentrations and plankton biomass consistently being available at these time scales (O(days)).

Although the DSI insertion results in only a temporary improvement in simulation skill for PP, P, Z, and A, there is a relatively long-term improvement in the simulation skill of nitrate (Fig. 3e). Whereas plankton biomass and ammonium concentration are governed by biological processes with time scales of O(1 day), nitrate concentration is largely determined by physical (advective) processes with much longer time scales. The nitrate simulation, therefore, remains dependent on the initial condition for a much longer period of time. The continual reinitialization of the model via data insertion thus provides a significant improvement to the overall simulation skill of nitrate, whereas any improvement for phytoplankton, zooplankton or ammonium is short-lived.

In a second experiment, Data Set II (synthetic ocean color data) is inserted into the FH01 model. As expected, $\Psi_P = 0$ at the specific times when observations are inserted into the model (Fig. 3b); however, on alternate days when data are not available, values of Ψ_P are just as high as the *a priori* misfits (R_P) computed from the non-data assimilative simulation. For the year of 1992, the DSII insertion results in an average reduction in

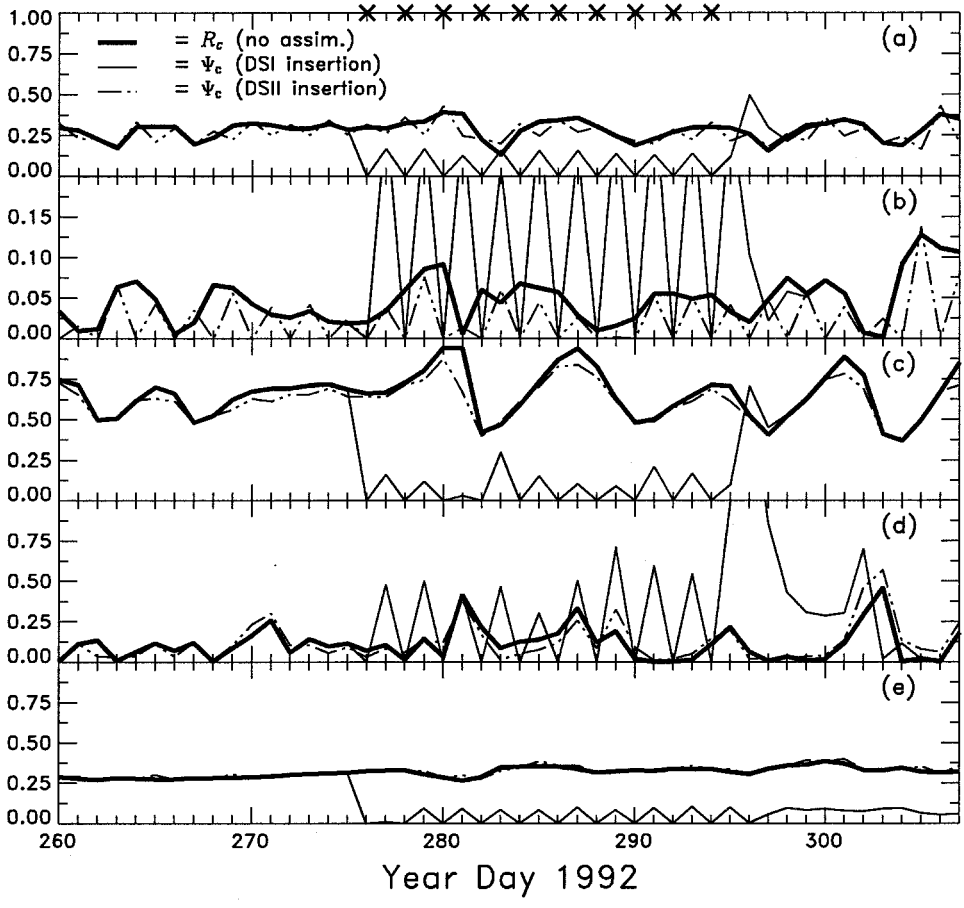

Figure 3. Comparison of model-data misfits generated without data assimilation ($R_C(t)$; thick line), with the insertion of DSI (solid line), and with the insertion of DSII (dot-dash line) for (a) primary production, (b) phytoplankton, (c) zooplankton, (d) ammonium, and (e) nitrate. Specific times of DSI insertion are denoted by **x**; DSII insertion occurs every other day throughout 1992. Note the change in y-axis scale in (b).

model data misfit for phytoplankton from 0.06 to 0.02, and little or no improvement in the simulation skill of the remaining model components. In fact, over this time period the simulation skill of nitrate deteriorates from an *a priori* value of $R_N = 0.25$ to $\Psi_N = 0.29$. Furthermore, as soon as data are no longer inserted, there is a rapid convergence of the assimilation and no-assimilation time series: for example, only seven days after the last ocean color data point is inserted, the post-assimilation misfit (Ψ_C) and *a priori* misfit (R_C) are indistinguishable.

ii. Variational adjoint method. When DSI (synthetic cruise data) is assimilated using the adjoint method, the exact values of the model control variables are perfectly recovered.

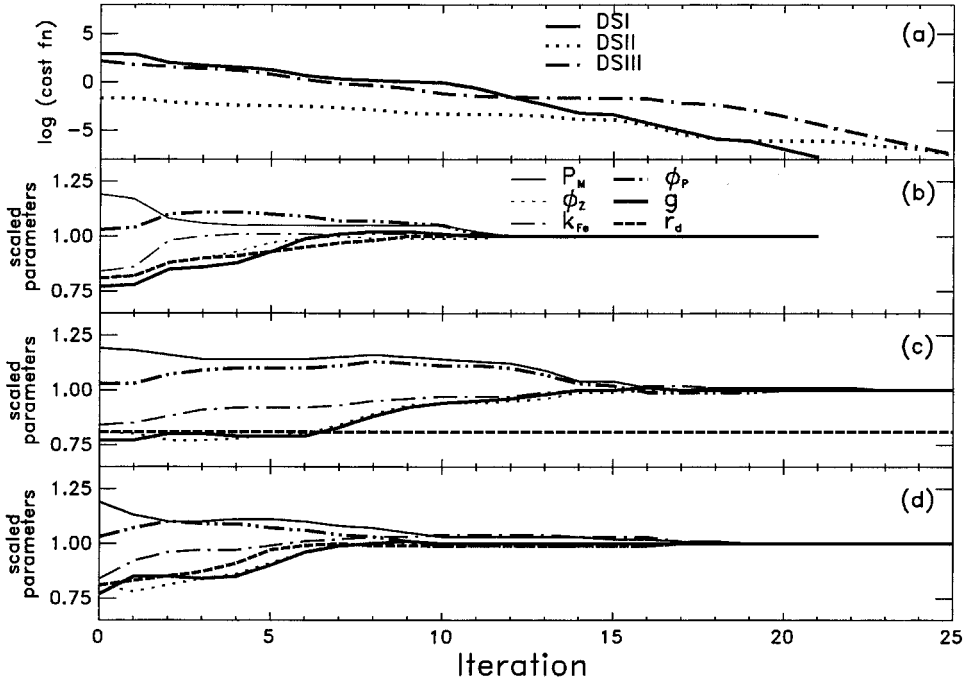

Figure 4. (a) Value of the cost function as a function of iteration number for the adjoint assimilation of DSI, DSII and DSIII (a), and values of the scaled model control variables as a function of the number of iterations for the assimilation of DSI (b), DSII (c), and DSIII (d).

The cost function is reduced from $O(10^3)$ to $O(10^{-8})$ in roughly 25 iterations (Fig. 4a), and the six model control variables are recovered nearly simultaneously (Fig. 4b). Forty-nine additional twin experiments are conducted in which the scaled model control variables are randomly assigned different initial values within their respective *a priori* ranges (Table 3). In each case the same values of the control variables are recovered, indicating that the global minimum of the cost function has been identified. If the *a priori* ranges of the model control variables are tripled, perfect parameter recoveries are still possible, however the number of iterations required is roughly 50% larger. Similar results are also obtained when fewer data, e.g. 4 days of PP, P, Z, A, and N cruise data, are assimilated. When even fewer data are assimilated, multiple values for the model control variables are recovered, and it becomes increasingly difficult to identify the absolute minimum of the cost function.

The assimilation of DSII (synthetic ocean color data) results in the perfect recovery of five of the six control variables in all fifty numerical experiments; however, the value of the recycling parameter (r_D) always remains unchanged (Fig. 4c). Because primary production and plankton concentrations are independent of the value assigned to r_D, the assimilation of a data set that does not include nutrient concentrations cannot

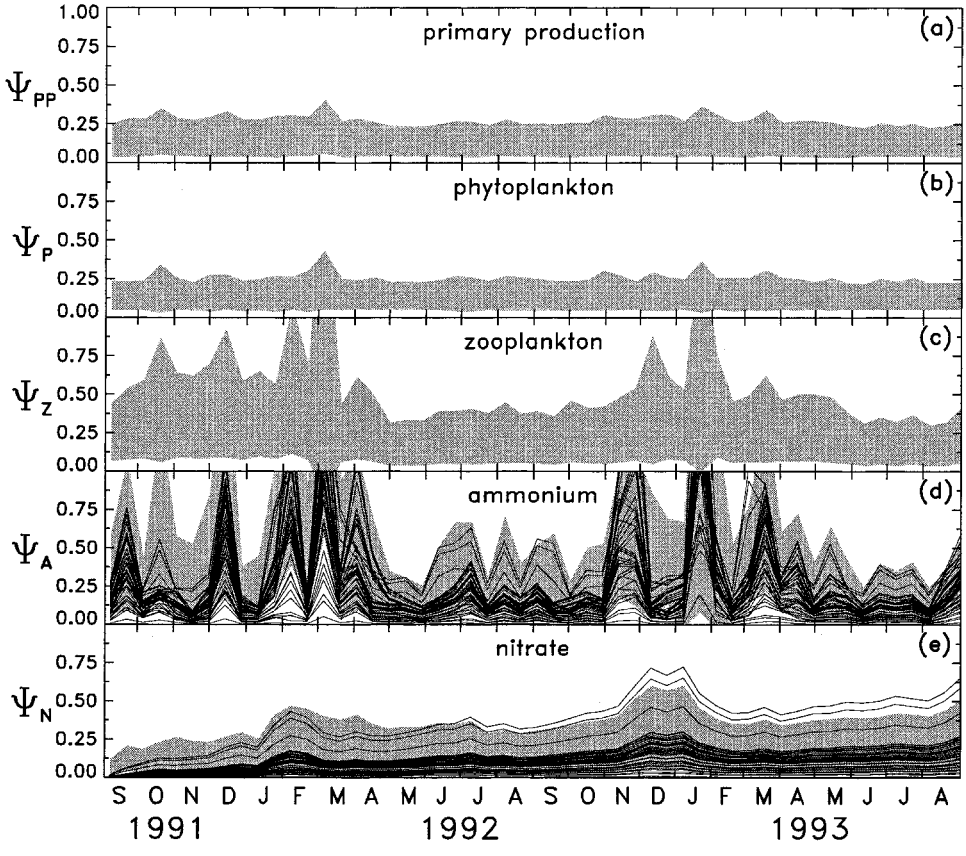

Figure 5. Time series of (a) $\Psi_{PP}(t)$, (b) $\Psi_P(t)$, (c) $\Psi_Z(t)$, (d) $\Psi_A(t)$, and (e) $\Psi_N(t)$ averaged over 14 days, generated using parameter sets recovered via the adjoint assimilation of DSII. Results are shown for 50 different *a priori* estimates of the control variables. In (a), (b) and (c), misfits are always equal to zero. Shaded regions indicate plus and minus one standard deviation of the mean of the fifty reference (no assimilation) time series, $R_C(t)$.

recover any information on r_D. As a result, these assimilation experiments result in simulated time series of PP, P, and Z that exactly reproduce the data, whereas the simulated time series of ammonium and nitrate, which depend heavily on the value assigned to r_D, produce misfits that show little improvement over their pre-assimilation values (Fig. 5).

The assimilation of DSIII, which supplements DSII with two days of PP, P, Z, A, and N cruise data, results in the perfect recovery of all six control variables (Fig. 4d), and hence $\Psi_{PP}(t) = \Psi_P(t) = \Psi_Z(t) = \Psi_A(t) = \Psi_N(t) = 0$. Further experimentation reveals that perfect parameter recoveries are also possible even if only 3 months, rather than six months, of phytoplankton data are supplemented with two days of cruise data.

Table 5. Summary of variation in scaled control variables recovered from assimilation of DSI with 20% random noise. Values of 1.00 indicate perfect parameter recoveries.

Realization	P'_M	φ'_Z	k'_{Fe}	φ'_P	g'	r'_D
1	1.01 ± 0.04	0.98 ± 0.01	0.98 ± 0.03	1.11 ± 0.04	0.95 ± 0.02	0.99 ± 0.03
2	0.99 ± 0.04	1.05 ± 0.02	1.00 ± 0.03	0.98 ± 0.05	1.06 ± 0.02	1.04 ± 0.03
3	0.91 ± 0.04	0.99 ± 0.01	1.06 ± 0.03	0.81 ± 0.04	0.96 ± 0.02	0.97 ± 0.02
4	0.99 ± 0.04	0.98 ± 0.01	0.96 ± 0.03	1.00 ± 0.04	0.89 ± 0.02	0.95 ± 0.02
5	0.95 ± 0.04	1.01 ± 0.02	0.99 ± 0.03	1.05 ± 0.04	0.98 ± 0.02	0.93 ± 0.02
6	0.93 ± 0.04	1.01 ± 0.01	1.03 ± 0.03	0.83 ± 0.04	1.00 ± 0.02	1.00 ± 0.03
7	0.90 ± 0.03	1.06 ± 0.02	1.02 ± 0.03	0.85 ± 0.04	1.06 ± 0.03	1.00 ± 0.03
8	1.14 ± 0.06	0.97 ± 0.02	1.01 ± 0.03	1.21 ± 0.05	1.00 ± 0.02	0.96 ± 0.03
9	0.96 ± 0.04	0.95 ± 0.01	1.05 ± 0.03	0.89 ± 0.04	0.98 ± 0.02	0.98 ± 0.03
10	0.81 ± 0.03	1.01 ± 0.02	0.94 ± 0.03	0.86 ± 0.04	1.02 ± 0.03	0.88 ± 0.02
Mean percent error over ten realizations*	7%	3%	3%	12%	4%	4%

*Mean percent error over ten realizations is computed as: $100 \sum_{j=1}^{10} |y_j - 1.0|/10$ where the y_j are the ten realizations of each scaled control variable.

b. Variational adjoint assimilation of imperfect data

In the numerical twin experiments described thus far, the synthetic data have been perfectly consistent with the model dynamics; however, in reality inconsistencies between data and model arise from observational errors, including misfits due to subsampling spatially variable fields, as well as missing model dynamics. To examine the ramifications of such inconsistencies, numerical experiments are conducted with data containing various levels of random noise and bias.

i. Data with random noise. Twenty percent random noise is added to Data Set I and Data Set III, and the resulting noisy data are assimilated via the adjoint method in separate assimilation experiments. Because this procedure involves random errors, multiple experiments will not produce identical results. Therefore, ten realizations (each consisting of fifty experiments) are performed for both DSI and for DSIII, in which different random errors, always with a maximum magnitude of 20%, are added to the synthetic data. For each realization, the same fifty sets of initial values are used for the control variables; however, all fifty experiments always result in the recovery of the same parameter set, indicating that the global minimum of the cost function is successfully identified in each realization.

Recovered values of the scaled control variables differ from those used to generate the true model simulation. The mean differences between the recovered and true values is about 5% for the assimilation of *in situ* cruise data (Table 5), and 9% for the assimilation of ocean color data (Table 6), suggesting that the long (six months) time series of phytoplankton chlorophyll does not make up for having only two days (as opposed to ten days) of cruise data available for the remaining model components. The greatest departures between the true and recovered values occur for P'_M, φ'_P, and k'_{Fe}. Although the assimilation of DSI yields errors in the recovery of k'_{Fe} of only 3% (Table 5), the assimilation of DSIII results in average errors in k'_{Fe} of 19% (Table 6). The error in the recovery of P'_M is also twice as great for the DSIII assimilation (14% versus 7%), whereas

Table 6. Summary of variation in scaled control variables recovered from assimilation of DSIII with 20% random noise. Values of 1.00 indicate perfect parameter recoveries.

Realization	P'_M	φ'_Z	k'_{Fe}	φ'_P	g'	r'_D
1	1.25 ± 0.09	1.03 ± 0.03	1.18 ± 0.02	1.06 ± 0.11	1.03 ± 0.06	1.00 ± 0.06
2	1.11 ± 0.11	0.91 ± 0.03	1.19 ± 0.19	0.91 ± 0.02	0.95 ± 0.01	0.90 ± 0.004
3	0.88 ± 0.06	0.99 ± 0.04	0.81 ± 0.08	1.05 ± 0.09	1.01 ± 0.05	1.03 ± 0.05
4	1.09 ± 0.15	0.94 ± 0.05	1.09 ± 0.19	0.95 ± 0.12	0.94 ± 0.05	0.97 ± 0.04
5	0.92 ± 0.12	0.96 ± 0.03	0.94 ± 0.13	0.98 ± 0.05	0.98 ± 0.03	1.02 ± 0.06
6	1.09 ± 0.10	1.04 ± 0.02	1.07 ± 0.10	1.03 ± 0.06	1.03 ± 0.01	0.97 ± 0.03
7	1.05 ± 0.13	1.00 ± 0.07	1.18 ± 0.23	0.90 ± 0.13	0.99 ± 0.08	0.97 ± 0.03
8	0.75 ± 0.04	0.99 ± 0.03	0.54 ± 0.02	1.20 ± 0.06	1.02 ± 0.04	1.19 ± 0.04
9	0.78 ± 0.10	1.06 ± 0.08	0.70 ± 0.08	1.09 ± 0.13	1.13 ± 0.09	1.12 ± 0.08
10	1.16 ± 0.01	0.96 ± 0.01	1.20 ± 0.10	0.99 ± 0.02	0.96 ± 0.02	0.98 ± 0.01
Mean percent error over ten realizations*	14%	4%	19%	7%	4%	6%

*Mean percent error over ten realizations is computed as: $100 \sum_{j=1}^{10} |y_j - 1.0|/10$ where the y_j are the ten realizations of each scaled control variable.

the error in the recovery of φ'_P is smaller for the DSIII assimilation (7% versus 12%). An examination of the model sensitivity results (Table 2) reveals that variations in these three parameters have similar effects on the model components; e.g., all significantly affect zooplankton biomass, but have very little impact on phytoplankton abundance. This is an indication that these parameters are probably correlated, resulting in relatively poor parameter recoveries with correspondingly high levels of uncertainty.

The inexact recovery of parameter values (Tables 5 and 6) leads to time series of $\Psi_C(t)$ that are no longer identically equal to zero. When the noisy version of Data Set I is assimilated (Fig. 6), the average misfits for the ten realizations are computed to be: $\langle\overline{\Psi_{PP}}\rangle = 0.04$, $\langle\overline{\Psi_P}\rangle = 0.02$, $\langle\overline{\Psi_Z}\rangle = 0.07$, $\langle\overline{\Psi_A}\rangle = 0.13$, and $\langle\overline{\Psi_N}\rangle = 0.03$. These values are 2–8 times smaller than the corresponding $\langle\overline{R_c}\rangle$ values obtained for the reference (no assimilation) simulations. Thus, even when noisy observations are assimilated using the adjoint method, simulation skill is still substantially improved.

Although values of $\Psi_{PP}(t)$, $\Psi_P(t)$, and $\Psi_N(t)$ are low (typically less than 0.05; Fig. 6), values of $\Psi_A(t)$ are greater, at times exceeding 1.0. These high values occur because ammonium can undergo large (order of magnitude) changes in concentration on very short time scales (O(days); FH01, their Fig. 8). As a result, small changes in event timing can cause large changes in the values of $\Psi_A(t)$. In contrast, the characteristic time scales of chlorophyll and nitrate are longer (FH01), and thus small changes in event timing do not cause large values of $\Psi_P(t)$ or $\Psi_N(t)$.

Experiments with other levels of random noise (0–40%) are also performed for both DSI and DSIII, as well as a combination of Data Sets I and III (Fig. 7a–e). Values of $\langle\overline{\Psi_c}\rangle$ increase nearly linearly for all model components as the magnitude of random noise added to the synthetic data is increased. Because the ocean color data set (DSIII) contains more plankton data and fewer nutrient data than the cruise data set (DSI), the assimilation of noisy ocean color data results in values of $\langle\overline{\Psi_{PP}}\rangle$ and $\langle\overline{\Psi_P}\rangle$ which are 40% lower than those obtained via the assimilation of noisy *in situ* cruise data, whereas $\langle\overline{\Psi_A}\rangle$ and $\langle\overline{\Psi_N}\rangle$ are

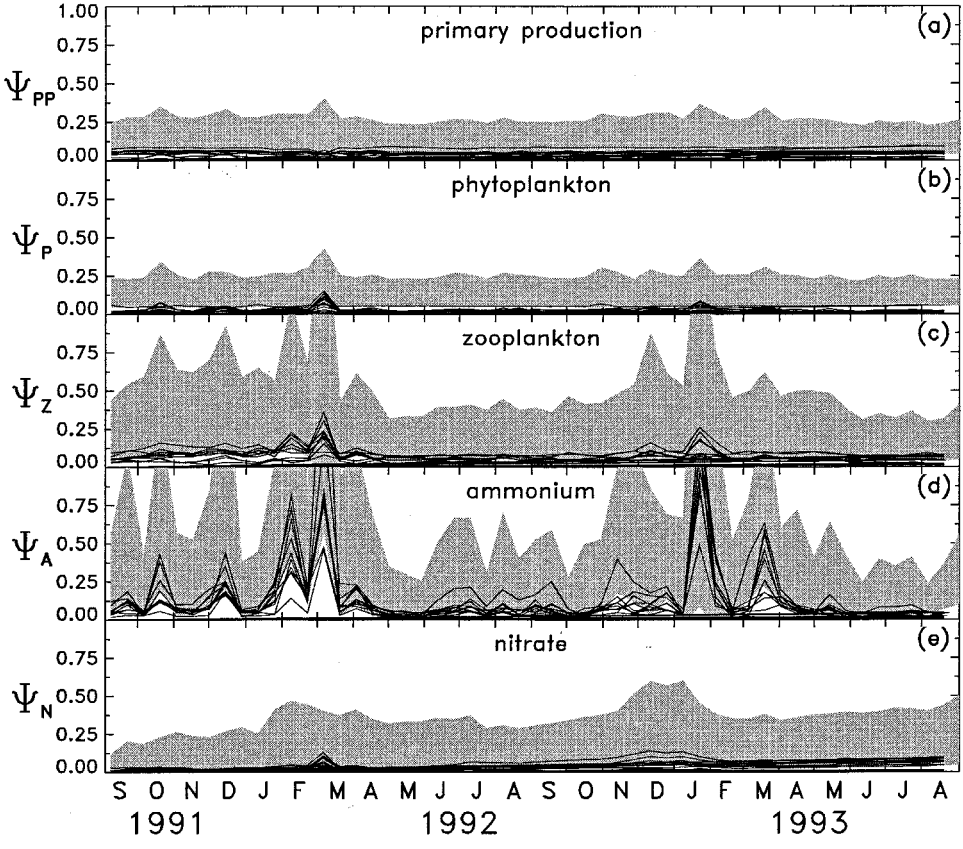

Figure 6. Time series of (a) $\Psi_{PP}(t)$, (b) $\Psi_P(t)$, (c) $\Psi_Z(t)$, (d) $\Psi_A(t)$, and (e) $\Psi_N(t)$ averaged over 14 days, for simulations generated using parameter sets recovered via the adjoint assimilation of Data Set I to which 20% random noise has been added. Ten random realizations are shown, as described in text. Shading represents plus and minus one standard deviation of the mean of the fifty reference (no assimilation) time series, $R_C(t)$.

nearly twice as high when the ocean color data are assimilated in place of the cruise data. Not surprisingly, the highest simulation skill and lowest misfits are obtained if Data Sets I and III are both assimilated simultaneously. In this case $\langle\overline{\Psi_{PP}}\rangle$ and $\langle\overline{\Psi_P}\rangle$ are nearly identical to those obtained for the DSIII assimilation case, whereas $\langle\overline{\Psi_Z}\rangle$, $\langle\overline{\Psi_A}\rangle$ and $\langle\overline{\Psi_N}\rangle$ are even lower than those of the DSI assimilation case (Fig. 7a–e).

When high levels of random noise (>30%) are added to the synthetic data prior to assimilation, multiple minima of the cost function are found; i.e., the same parameter set is *not* recovered for all 50 initial estimates of the control variables. (Results shown in Figure 7 represent those associated with the most commonly occurring parameter set.) Even though multiple minima are occurring when 40% random noise is added to the assimilated data, a doubling of random noise from 20% to 40% is generally still associated with a doubling in

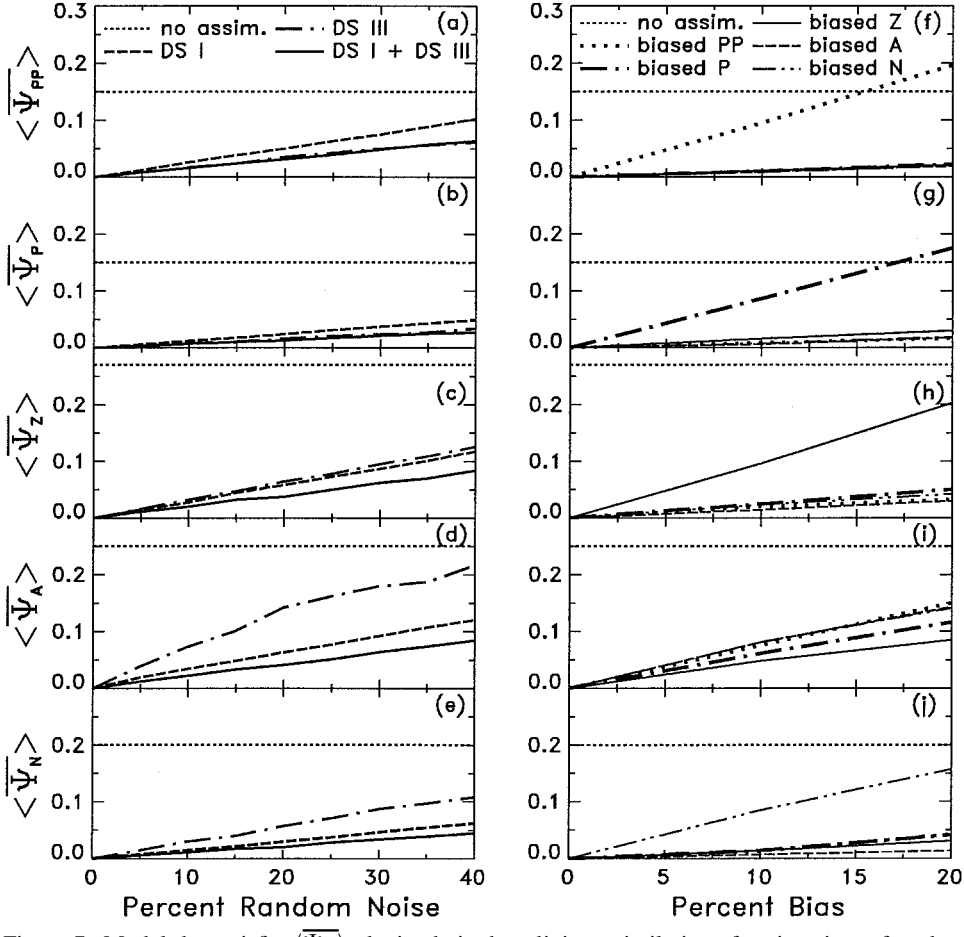

Figure 7. Model-data misfits $\langle\overline{\Psi_C}\rangle$ obtained via the adjoint assimilation of various imperfect data sets. (a) $\langle\overline{\Psi_{PP}}\rangle$, (b) $\langle\overline{\Psi_P}\rangle$, (c) $\langle\overline{\Psi_Z}\rangle$, (d) $\langle\overline{\Psi_A}\rangle$, and (e) $\langle\overline{\Psi_N}\rangle$ are shown as a function of the percent random noise added to the synthetic data: DSI (dotted line), DSIII (dash-dot line), and both DSI and DSIII (solid line). Model-data misfits (f) $\langle\overline{\Psi_{PP}}\rangle$, (g) $\langle\overline{\Psi_P}\rangle$, (h) $\langle\overline{\Psi_Z}\rangle$, (i) $\langle\overline{\Psi_A}\rangle$, and (j) $\langle\overline{\Psi_N}\rangle$ are shown as a function of the percent bias added individually to the five components of DSI. Model-data misfits obtained without data assimilation, $\langle\overline{R_C}\rangle$ (dotted lines), are included for reference.

the magnitudes of each $\langle\overline{\Psi_c}\rangle$ component. The one exception is the nonlinearity in $\langle\overline{\Psi_A}\rangle$ for the Data Set III assimilation case, which is most likely due to these multiple minima.

ii. Biased data. In addition to random errors, observations are typically also associated with a certain degree of bias. Depending on the type of observation, (e.g., rate, plankton biomass, or nutrient concentration) and the observational platform from which the data are collected, (e.g., satellite or ship) varying levels of bias may be present. In order to

Table 7. Summary of variation in scaled control variables recovered from assimilation of data sets with varying levels of bias. Values of 1.00 indicate perfect parameter recoveries.

Bias	Data set	Component	P'_M	φ'_Z	k'_{Fe}	φ'_P	g'	r'_D	Mean param. error*
−20%	I	*PP*	0.70 ± 0.02	1.01 ± 0.01	1.05 ± 0.04	0.55 ± 0.03	1.00 ± 0.02	0.93 ± 0.03	15%
20%	I	*PP*	1.27 ± 0.04	0.99 ± 0.01	0.87 ± 0.02	1.45 ± 0.06	1.00 ± 0.02	0.97 ± 0.02	15%
−20%	I	*P*	1.43 ± 0.07	0.90 ± 0.02	1.00 ± 0.03	1.40 ± 0.09	1.33 ± 0.06	1.08 ± 0.04	22%
20%	I	*P*	0.76 ± 0.03	1.07 ± 0.01	0.97 ± 0.03	0.76 ± 0.03	0.79 ± 0.02	0.88 ± 0.02	15%
−20%	I	*Z*	0.95 ± 0.04	1.08 ± 0.02	0.93 ± 0.03	1.14 ± 0.05	1.12 ± 0.03	0.93 ± 0.03	9%
20%	I	*Z*	1.03 ± 0.04	0.94 ± 0.01	1.05 ± 0.03	0.85 ± 0.04	0.91 ± 0.02	1.06 ± 0.03	7%
−20%	I	*A*	1.18 ± 0.05	0.98 ± 0.02	1.21 ± 0.03	0.97 ± 0.05	1.00 ± 0.03	0.86 ± 0.03	10%
20%	I	*A*	0.85 ± 0.03	1.01 ± 0.02	0.83 ± 0.02	0.99 ± 0.04	0.98 ± 0.02	1.15 ± 0.03	9%
−20%	I	*N*	0.87 ± 0.02	0.98 ± 0.02	0.86 ± 0.02	1.01 ± 0.03	0.97 ± 0.02	0.80 ± 0.02	9%
20%	I	*N*	1.10 ± 0.12	1.06 ± 0.03	1.10 ± 0.07	0.98 ± 0.08	1.05 ± 0.03	1.22 ± 0.16	9%
−20%	I	*PP*, *P*, *Z*, *A*, *N*	1.02 ± 0.05	0.98 ± 0.02	1.10 ± 0.03	1.00 ± 0.06	1.49 ± 0.07	0.68 ± 0.02	16%
20%	I	*PP*, *P*, *Z*, *A*, *N*	0.96 ± 0.03	1.04 ± 0.01	0.89 ± 0.02	0.99 ± 0.03	0.73 ± 0.01	1.34 ± 0.04	14%
−20%	III	*P*	1.03 ± 0.12	0.92 ± 0.05	0.82 ± 0.09	1.24 ± 0.12	1.40 ± 0.09	0.97 ± 0.07	16%
20%	III	*P*	0.90 ± 0.09	1.06 ± 0.04	1.01 ± 0.11	0.88 ± 0.02	0.77 ± 0.02	1.18 ± 0.05	12%

*Mean parameter error is computed as: $100/6 \sum_{i=1}^{6} |x_i - 1.0|$ where the x_i are the values of the six scaled control variables.

investigate the potential problems associated with assimilating data containing biased errors, numerical experiments are conducted in which +20% and −20% biases are added to the *PP* component of DSI, while the *P*, *Z*, *A*, and *N* data are assumed to be error-free. Experiments are also carried out in which these biases are added individually to the other components of DSI (*P*, *Z*, *A*, *N*), as well as to all five data components simultaneously. In a final experiment, biases are added to the synthetic ocean color observations of DSIII. In each of these cases, fifty numerical experiments are carried out with different initial random estimates for the model control variables. When highly biased data (20%) are assimilated, multiple minima of the cost function can exist; results associated with the most commonly occurring minimum are presented.

When biases are added to the assimilated data sets, often the model control variables are no longer perfectly recovered. Because of nonlinearities associated with the model equations, a bias of a certain percentage typically does not result in errors in the recovered parameter values of the same magnitude. However, in general the assimilation of positively and negatively biased data tends to alter the values of the recovered parameters by roughly an equal magnitude, but in the opposite direction (Table 7). For example, if the *PP* component of DSI is biased by −20%, the recovered value of P'_M is 0.70, i.e. a decrease of 30% from the true value of 1.00. An analogous *PP* bias of +20% results in an *increase* in P'_M of nearly the same magnitude, such that the final value of P'_M is 1.27 (Table 7).

Although the assimilation of biased *PP* data results in the imperfect recovery of P'_M and φ'_P by 30% and 45% respectively, other parameters, such as those governing zooplankton biomass (g' and φ'_Z), are successfully recovered. If the biases are added to the *P* component of DSI instead of to the *PP* data, not only are P'_M and φ'_P poorly recovered, but the value of g' is associated with a 33% error as well. When biases are added to ammonium or nitrate data, φ'_Z, φ'_P, and g' are successfully recovered; however, values of P'_M, k'_{Fe}, and r'_D are in error by 10–20%. If biases are added simultaneously to all five components of

DSI, g' and r'_D are associated with errors as large as 30–50%. Overall, the poorest parameter recoveries occur if biases are added to phytoplankton data, suggesting that the simulation results are most highly dependent on this model component. Thus it is crucial for observational programs to attain high quality chlorophyll measurements, since phytoplankton time series are of central importance to attaining accurate model simulations.

The imperfect parameter recoveries resulting from the assimilation of biased data can lead to large model-data misfits. In general, the magnitudes of these misfits are linearly dependent on the magnitude of bias added to the synthetic data (Fig. 7f–j). For example, if a 10% bias is added to the primary production component of DSI and the resulting time series is assimilated along with perfect time series of P, Z, A, and N, the resulting value of $\langle\overline{\Psi_{PP}}\rangle$ is 0.10. If a 20% bias is assumed and the same assimilation experiment is performed, $\langle\overline{\Psi_{PP}}\rangle$ doubles in magnitude to 0.20 (Fig. 7f). Generally the greatest values of $\langle\overline{\Psi_C}\rangle$ occur when a bias exists in model component C; however, this is not true for ammonium. The assimilation of biased N data results in a poor recovery of r_D, to which the concentration of ammonium is particularly sensitive (Table 2). The assimilation of biased PP data also strongly affects ammonium concentration, since regenerated production (a primary term in the ammonium conservation equations; see the Appendix) is a strong function of PP. Thus biases in PP and N cause just as large a deterioration in the simulation skill of A, as do biases in the ammonium data itself.

c. *Sampling strategies*

Successful parameter recoveries are dependent not only on observational errors, but also on the amount of available data. The degree of spatial and temporal averaging of the data may also affect the success of assimilative model runs. Numerical twin experiments are performed in order to examine the potential magnitude of these effects.

i. Data availability. As discussed earlier, if 20% noise is added to DSI (a 20 day time series) prior to assimilation, imperfect model control variables are recovered, and values of $\langle\overline{\Psi_C}\rangle$ range between 0.02 and 0.07 (Fig. 7b,d). If, however, only a 6-day (10-day) time series of noisy cruise data is available for assimilation, model-data misfits are significantly higher (Fig. 8a), ranging from $\langle\overline{\Psi_P}\rangle = 0.06$ (0.03) to $\langle\overline{\Psi_A}\rangle = 0.13$ (0.09). If longer time series are available for assimilation (e.g. 40 days), the deterioration in simulation skill due to the addition of random noise is substantially reduced, with $\langle\overline{\Psi_C}\rangle < 0.05$ for all model components. Thus, when random noise is present in the data, the increase in time series length from 6 days to 40 days can provide a large (70%) improvement in simulation skill. A large percentage of this improvement occurs if 10 days rather than 6 days of data are assimilated. This is because of the strong 6–8 day variability of the equatorially trapped internal gravity waves (FH01). Further improvement results if the strong tropical instability wave signal (20–30 day) is resolved by assimilating at least 40 days of data.

If biased errors are individually added to each component of DSI, an increase in the number of days of data that are assimilated produces little change in simulation skill

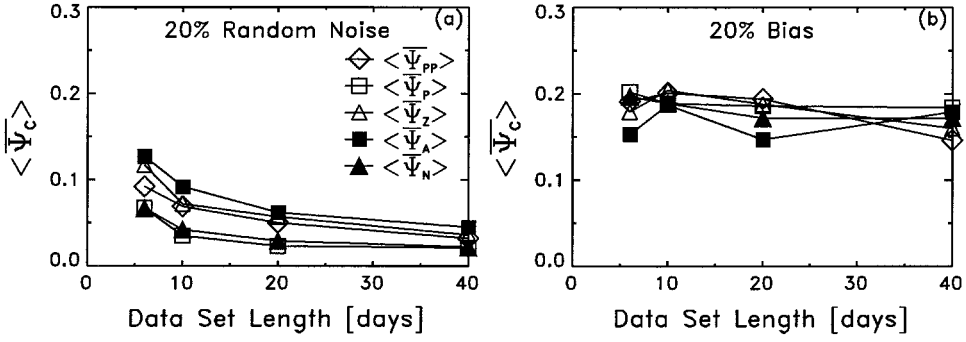

Figure 8. Model-data misfits, $\langle \overline{\Psi_C} \rangle$, as a function of the length of the assimilated synthetic cruise data time series. In (a) $\langle \overline{\Psi_C} \rangle$ is computed after 20% random noise is added simultaneously to PP, P, Z, A, and N, and in (b) each $\langle \overline{\Psi_C} \rangle$ is computed after 20% bias is added only to component C of the synthetic cruise data time series.

(Fig. 8b). However, simulation skill can depend on the particular days on which data are assimilated. For example, the relatively large value of $\langle \overline{\Psi_A} \rangle$ associated with the 10-day time series as compared to the 6-day time series (Fig. 8b), is reduced if data from YD286 to YD296 are assimilated in place of data from YD276 to YD286. This is primarily because of the large peaks in P, Z, and A concentrations occurring between YD282–285 (FH01); in contrast, concentrations during YD286–296 are more stable, resulting in lower assimilation errors.

A similar set of twin experiments is also conducted for ocean color data (Fig. 9). If no random noise is added to the synthetic data, a 90-day time series supplemented by two days of *in situ* data provides sufficient information such that the control variables are recovered exactly; however, if 20% random noise is present in the 90-day assimilated time series, imperfect values of the control variables are recovered, resulting in model-data misfits

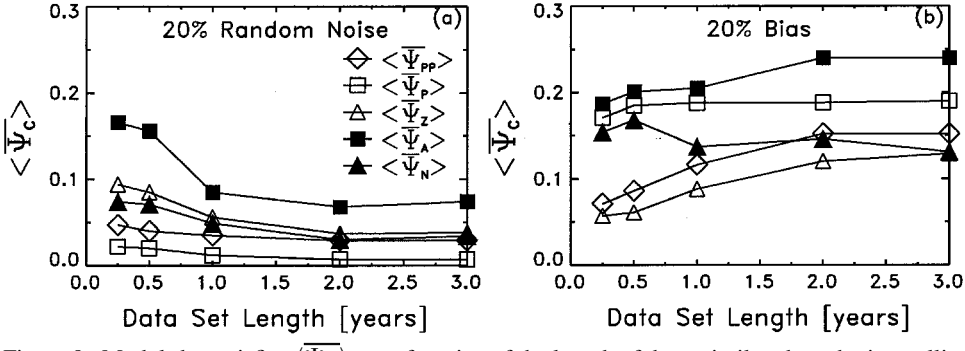

Figure 9. Model-data misfits, $\langle \overline{\Psi_C} \rangle$, as a function of the length of the assimilated synthetic satellite ocean color time series. In (a) 20% random noise is added, and in (b) 20% bias is added to the synthetic data.

Table 8. Average misfits ($\langle\overline{\Psi_c}\rangle * 100$) as a function of cruise length and sampling strategy of DSI. Results represent means and standard errors of ten realizations assuming a random noise level of 20%.

Length of *in situ* cruise data set	Sampling strategy	$\langle\overline{\Psi_{PP}}\rangle$	$\langle\overline{\Psi_P}\rangle$	$\langle\overline{\Psi_Z}\rangle$	$\langle\overline{\Psi_A}\rangle$	$\langle\overline{\Psi_N}\rangle$
20 days	*PP*, *P*, *Z*, *A*, *N* every other day	4.1 ± 0.4	3.2 ± 0.2	5.7 ± 0.4	6.7 ± 0.2	3.5 ± 0.3
20 days	*PP*, *P*, *Z*, *A*, *N* every day	2.8 ± 0.2	2.4 ± 0.2	3.4 ± 0.3	5.1 ± 0.3	2.2 ± 0.2
10 days	*PP*, *P*, *Z*, *A*, *N* every day	3.5 ± 0.3	3.2 ± 0.3	4.6 ± 0.4	7.0 ± 0.3	3.3 ± 0.3
20 days	*PP*, *P*, *Z* every other day *A*, *N* every day	3.7 ± 0.3	3.0 ± 0.2	5.1 ± 0.4	5.7 ± 0.2	2.4 ± 0.2

ranging between $\langle\overline{\Psi_A}\rangle = 0.17$ to $\langle\overline{\Psi_P}\rangle = 0.02$ (Fig. 9a). As the assimilated time series is lengthened, values of $\langle\overline{\Psi_C}\rangle$ decrease. Because there is significant energy in the temperature forcing fields at a period of 10–12 months, a dramatic decrease in model-data misfit results if a year of ocean color data are assimilated rather than six months. There is no additional improvement in simulation skill if more than two years of data are assimilated.

In contrast, if biased ocean color data are assimilated, there is no improvement in simulation skill as longer and longer time series become available (Fig. 8b). If the assimilated time series is lengthened from three months to three years, model-data misfits for primary production and zooplankton more than double and misfits for ammonium increase by 30%. The simulation skill of phytoplankton is nearly independent of how many days of data are assimilated, and is always poorer than the *a priori* (nonassimilative) case ($\langle\overline{R_P}\rangle = 0.15$). Although model-data misfits for nitrate are slightly reduced as more biased ocean color data are assimilated, in general assimilating *more* biased data does not necessarily improve simulation skill, and may even *increase* model-data misfits.

Numerical twin experiments are also used to examine the effects of altering the frequency at which data are assimilated. For instance, if cruise data are assimilated every day as opposed to every other day, simulation skill is improved by 25%–40% (Table 8). If the total number of observations is held constant, but data are available every day for 10 days as opposed to every other day for 20 days, there is no significant change in simulation skill, with the possible exception of zooplankton (4.6 ± 0.4 versus 5.7 ± 0.4). During the JGOFS EqPac experiment, nutrient data were generally collected at least once a day, whereas primary production and plankton data were obtained once every other day. This higher frequency of nutrient data collection improves the simulation skill of *A* (15%) and *N* (31%) as would be expected; however, this increased nutrient sampling frequency does not significantly affect the simulation skill of *PP*, *P*, or *Z* (Table 8).

A combination of satellite position and cloud cover causes SeaWiFS ocean color data in the central equatorial Pacific to be available about 50% of the time; i.e., approximately every other day. Twin experiments demonstrate that assimilating ocean color data every

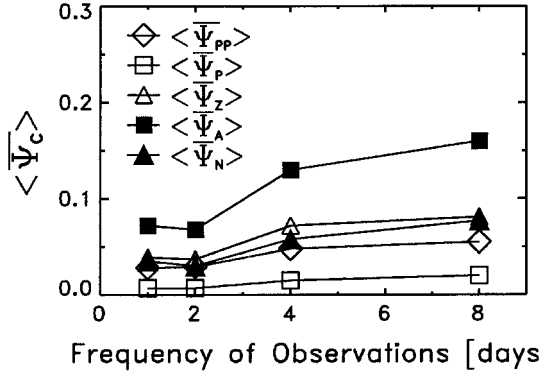

Figure 10. Model-data misfits, $\langle\overline{\Psi_C}\rangle$, as a function of the frequency for which the assimilated satellite ocean color data are available. In each case 20% random noise has been added to a two-year long synthetic data time series.

day, as opposed to every other day, does not reduce model-data misfit; however, if data are assimilated every 4 days instead of every 2 days, a large deterioration in simulation skill occurs for most model components (Fig. 10).

ii. Assimilating SeaWiFS composites. Ocean color satellite data are typically available as a time series of composites, where each composite is computed as the average of all data falling within a specified spatial and temporal range. SeaWiFS data, for example, are routinely available as 8-day and monthly composites. In order to investigate the effect of assimilating composited data, as opposed to instantaneous (daily) data, four different synthetic ocean color time series are assimilated (each in addition to two days of cruise data): (i) instantaneous data once every 2 days (i.e. DSIII), (ii) instantaneous data once every 8 days, (iii) 8-day composites, and (iv) 4-day composites once every 8 days. Note that time series (ii)–(iv) all contain the same number of observations, whereas four times as many observations are available in DSIII (i).

Assuming no random noise nor biases are present, the assimilation of instantaneous data every two days or every eight days results in perfect parameter recoveries and $\langle\overline{\Psi_C}\rangle = 0$ (Fig. 11); however, if composites are assimilated in place of the instantaneous data, $\langle\overline{\Psi_C}\rangle$ may reach values as high as 0.15 even in the absence of any random noise or bias (Fig. 11d). Because random errors are partially averaged out in the formation of the composited time series, the addition of random noise to the synthetic ocean color data causes a larger deterioration in simulation skill for the instantaneous data time series, than for the composited data time series. For example, when random noise is added to the instantaneous data time series and the resulting data set is assimilated, model-data misfits increase substantially: values of $\langle\overline{\Psi_A}\rangle$ increase sharply from 0.00 to 0.16, and are no longer significantly different from the analogous values of $\langle\overline{\Psi_A}\rangle$ obtained using the composited data (Fig. 11d). In the presence of even higher noise levels (40%), the composited and

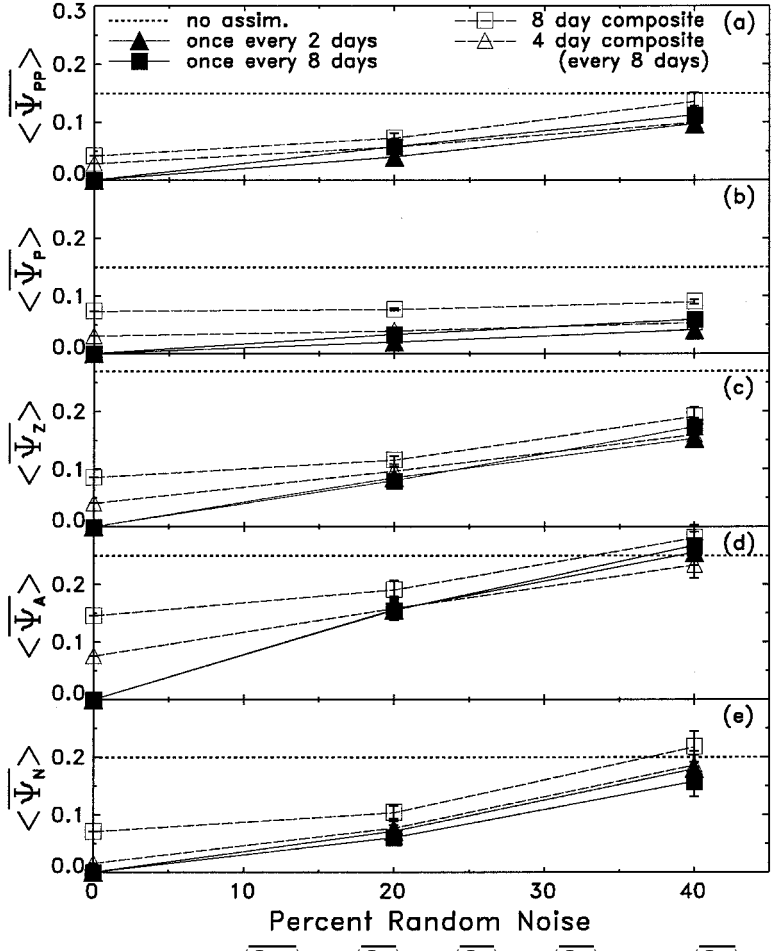

Figure 11. Model-data misfits (a) $\langle\overline{\Psi_{PP}}\rangle$, (b) $\langle\overline{\Psi_{P}}\rangle$, (c) $\langle\overline{\Psi_{Z}}\rangle$, (d) $\langle\overline{\Psi_{A}}\rangle$, and (e) $\langle\overline{\Psi_{N}}\rangle$ obtained via the assimilation of 180-day time series of composited and instantaneous (daily) ocean color data, shown as a function of the percent random noise added to the synthetic data. Model-data misfits obtained without data assimilation, $\langle\overline{R_C}\rangle$ (dotted lines), are shown for reference.

instantaneous assimilation results also become indistinguishable for $\langle\overline{\Psi_{PP}}\rangle$, $\langle\overline{\Psi_{Z}}\rangle$ and $\langle\overline{\Psi_{N}}\rangle$. Thus, even though the assimilation of error-free instantaneous data is more successful than the assimilation of error-free composited data, the assimilation of noisy composited data results in nearly as high simulation skill as the assimilation of noisy instantaneous data.

4. Discussion and summary

Although useful for many meteorological applications, simple data assimilation schemes such as data insertion may be insufficient for marine ecosystem models. Meteorological

models are typically highly dependent on initial conditions, and thus simple assimilation schemes which involve reinitializing the model whenever data become available can be quite successful in weather forecasting. Partially because of the short time scales of the dominant biological processes, lower trophic level marine ecosystem models quickly (within days) become independent of component initial conditions. As a result, in the numerical twin experiments conducted in this analysis, the assimilation and no-assimilation time series of plankton concentrations are indistinguishable only seven days after the last ocean color data point is inserted.

These results are consistent with those of Ishizaka (1990), who found that the insertion of satellite ocean color data into a physical-biological model of the southeastern U.S. continental shelf caused the simulated phytoplankton field to rapidly (within four days after the last assimilated observation) converge to the analogous fields obtained without assimilation. When biological processes were removed from the model, the assimilation and nonassimilation cases still converged within several days, suggesting that this rapid convergence was at least partially due to the short time scales of the physical processes associated with the Gulf Stream system. Similarly, in the present study equatorially-trapped internal gravity waves with periods of 6–8 days (FH01; Wunsch and Gill, 1976) may be effecting the rapid convergence of the assimilation/nonassimilation time series.

The success of data insertion thus depends on biological (plankton) and chemical (nutrient) observations being available at very frequent intervals (O(days)). The inception of remote-sensing ocean color sensors, such as SeaWiFS, now makes it possible to obtain surface chlorophyll data on these time scales. However, numerical experiment results (Fig. 3) indicate that successful simulations will require high frequency data on other model components as well. Currently there are no analogous high frequency measurements of zooplankton available on a global scale, and synoptic time series observations of nutrient concentrations such as ammonium and nitrate are rare.

The most serious disadvantage of applying schemes such as data insertion to marine ecosystem models, is that these types of methods assume an adequate knowledge of not only the model parameterizations, but also the model parameters. Ecosystem models are typically characterized by multiple empirical formulations for which parameter values are poorly known, and often unmeasurable. Simulations are often highly dependent on mortality rates, but these rates are difficult or impossible to measure and therefore poorly constrained. If inappropriate values are assigned to these parameters, simulation skill may be poor, even if data are inserted every other day (Fig. 3). Furthermore, it may be difficult to determine whether a failed simulation results from an inappropriate choice of parameter values, or whether there is an intrinsic error in model formulation. For example, nudging the Fasham *et al.* (1990) model toward ocean color observations causes ammonium concentrations to reach unrealistically high values (Armstrong *et al.,* 1995). Although altering the structure of the model to include multiple plankton size classes is one way to eliminate this pathological behavior (Armstrong *et al.,* 1995), it is possible that alternate

choices of parameters in the original Fasham *et al.* (1990) model also may reduce ammonium concentrations to realistic levels.

Although the variational adjoint method assumes that the model parameterizations are correct, specific values for each of the model parameters do not need to be precisely known as they do for data insertion. Results of identical twin experiments indicate that the adjoint method, which minimizes model-data misfits by adjusting model parameters, holds much promise for the assimilation of biological data into marine ecosystem models. For example, exact parameter recoveries are possible when assimilating synthetic data subsampled using the resolution of the JGOFS EqPac Time Series cruises (Fig. 4b). Exact parameter recoveries are also possible when synthetic ocean color data are assimilated along with a small amount (2 days) of nutrient, plankton and production data (Fig. 4d). Similarly promising results are also obtained when actual cruise and ocean color data at this resolution are assimilated into the FH01 ecosystem model using the variational adjoint method (Friedrichs, 2001). However, because it is possible that recovered parameter values may be offsetting either other parameter values that have remained fixed or inaccurate parameterizations, one may think of this parameter optimization procedure as a 'calibration' of the model, rather than an accurate determination of actual biological rate constants. The real utility of these simulations is not necessarily in identifying precise values of specific ecosystem parameters, but rather in knowing that the model has been calibrated to be reasonably consistent with the available data. As a result, we have greater faith in the other results and processes described by the model.

In the identical twin experiments described in this paper, data are generated by the model and thus the model and data are, by definition, entirely consistent. In reality, however, both observational errors in precision and accuracy as well as deficiencies in the model may cause simulated time series distributions to be inconsistent with observations. When this inconsistency is artificially reproduced by adding random noise to the synthetic data prior to assimilation, the adjoint method still improves simulation skill (Figs. 6, 7a–e). The presence of biases in the data, however, is more detrimental to the assimilation results (Fig. 7f–j). The addition of 20% bias to the phytoplankton component of the *in situ* cruise data causes errors of up to 43% in the values of the recovered control variables (Table 7), and high model-data misfits which exceed the *a priori* values computed without data assimilation (Fig. 7g). In contrast, the addition of 20% random noise to the same data set produces errors in the recovered control variables of only 3–12% (Table 5), and furthermore even when phytoplankton data associated with 40% random noise are assimilated, model-data misfits are still significantly reduced (Fig. 7b).

Biased errors are also particularly troublesome since increasing the duration over which biased data are available generally does not improve simulation skill (Figs. 8b, 9b). In fact, when assimilating biased ocean color data, increasing time series length from 6 months to 3 years causes a significant increase in model-data misfit (Fig. 9b). In contrast, when noisy data are assimilated, increasing the duration of the data time series improves simulation skill. Specifically, the largest improvement occurs if the cruise data time series is increased

from 6 days to 10 days (Fig. 8a), or the available satellite ocean color data time series is increased from 6 months to one year (Fig. 9a). This is because the time series of chlorophyll concentration has significant energy at periods ranging between 6–8 days and 6–12 months. In order to resolve high frequency processes such as equatorially-trapped internal gravity waves (FH01) and seasonal to annual variability, at least 10 days of cruise data and at least one year of ocean color data must be assimilated, respectively.

During the JGOFS EqPac cruises, plankton data were collected every other day for roughly 20 days; however, numerical twin experiments demonstrate that assimilating 10 days of data collected every day instead of 20 days of data collected every other day does not affect simulation skill (Table 8). Therefore, if it is possible to collect data on a daily basis as opposed to every other day, the length (and expense) of a cruise could be reduced or even halved. On the contrary, there appears to be no additional reduction in model-data misfit if ocean color data are assimilated every day as opposed to every other day. There is, however, a significant deterioration in simulation skill if data are available only every 4 days (Fig. 10). Thus, although typical cloud cover in the equatorial Pacific may not affect assimilation results, unusually cloudy weather associated with El Niño conditions may cause remotely-sensed ocean color data to be unavailable for days at a time, and hence simulation skill may be substantially reduced.

SeaWiFS data are typically available as 8-day and monthly composites; however, because the dominant time scales of marine ecosystems are typically on the order of days, the formation of these ocean color composites may produce time series that are inconsistent with biological observations. For example, a spectral analysis of the synthetic ocean color data reveals a spike in energy corresponding to a period of approximately 6 days, associated with equatorially trapped internal gravity waves (FH01). In the formation of an 8-day data composite, this energy spike is smeared out, causing an inconsistency between the model and composited data. As a result, the assimilation of this temporally-averaged data leads to relatively poor parameter recoveries. In contrast, 4-day composites at least partially resolve the internal gravity waves, and model-data misfits obtained after assimilating 4-day composite time series are typically less than half of those obtained for the 8-day composite assimilation (Fig. 11). If random noise is present in the data, however, the formation of the data composite will average out much of this noise, resulting in similar results for the assimilation of both the composited and instantaneous data (Fig. 11). Because real data are typically associated with significant random noise, it is anticipated that when actual observations are used (Friedrichs, 2001), the assimilation of composited data will be equally as successful as the assimilation of instantaneous data.

5. Future challenges

This analysis demonstrates that the variational adjoint method provides a successful means for combining biological and chemical oceanographic observations with marine ecosystem models, in order to improve simulation skill. Through the assimilation of synthetic cruise data based on the JGOFS EqPac experiment as well as synthetic SeaWiFS

ocean color data, it is possible to recover parameters governing processes such as grazing, growth, mortality and recycling. However, because high correlations exist between many model parameters, it is typically not possible to recover the entire parameter set with any degree of certainty (Matear, 1995; Prunet *et al.,* 1996a,b; Harmon and Challenor, 1997). Therefore, in this analysis the control variables consist of a subset of the model parameters. This results in the successful recovery of the control variables with low levels of uncertainty. A more robust and objective method would involve nondimensionalizing the model to obtain a parameter set containing a smaller number of uncorrelated parameters which could then be successfully recovered in its entirety. The feasibility of this approach is currently under investigation.

In the simple formulation of the cost function used in this analysis, there are no limitations on the values that the control variables may attain; i.e., there are no *a priori* penalties placed on these parameters. Although the initial parameter estimates are always within the uncertainty ranges of Table 3, there is no guarantee that the recovered optimal values will fall within these ranges. In certain experiments when very noisy observations are assimilated, seriously flawed parameter sets with errors exceeding 40% may be recovered. Despite these large errors, in certain cases the simulated time series generated from these flawed parameter sets may still agree reasonably well with the true time series. In these cases the model is tracking the data by misrepresenting key biological processes; because the amount of data assimilated in these experiments is small relative to the number of degrees of freedom, the model is poorly constrained and it may be possible for the model to reproduce the data without representing the correct dynamical processes. Thus when actual observations are assimilated (Friedrichs, 2001), it is important to be able to define reasonable error bounds on each of the model parameters, and either discard parameter estimates that fall outside these ranges or add penalties to the cost function to eliminate unrealistic parameter estimates.

As biological data sets, including *in situ,* satellite, and acoustic sources, continue to grow, data assimilative biological-physical models will play an increasingly crucial role in large multidisciplinary oceanographic observational programs. The research described here provides a framework for future global and basin-scale studies of biological data assimilation and predictive biogeochemical modeling; however there are still many questions which need to be addressed before biological-physical models are routinely data assimilative. For instance, an optimal method for assimilating both physical and biological data simultaneously is still under investigation. In this paper, the advantages and disadvantages of data insertion and the variational adjoint method were discussed independently; however, it is possible that these methods could be used as complimentary tools, where the adjoint could first be used to optimize the parameter values, and then nudging could be used to bring the simulation into even closer agreement with the data, if desired. Although the adjoint method is shown to be a very powerful technique for improving simulation skill through the combined use of data and models, it is not yet clear whether it is feasible to

apply this method to a fully three-dimensional coupled physical-biological model. Work toward this goal is currently underway.

Acknowledgments. I would like to thank Eileen Hofmann for the many helpful discussions and suggestions she provided throughout this work. The insightful comments of Paola Malanotte-Rizzoli and an anonymous reviewer are also greatly appreciated. The TAO Project Office, Michael J. McPhaden, Director, is thanked for the use of the extensive data available from their mooring array. Support for this work was provided by the National Aeronautics and Space Administration under grants NAGW-3550 and NCC-5-258. Computer resources and facilities were provided by the Center for Coastal Physical Oceanography at Old Dominion University. This is U.S. JGOFS Contribution #699.

APPENDIX

Ecosystem model equations

Each of the five model components (phytoplankton (P), zooplankton (Z), ammonium (A), nitrate (N), and detritus (D)) satisfies a general conservation equation of the form:

$$\frac{\partial \overline{C(t)}}{\partial t} = \overline{F_C(t)} + \overline{B_C(t)} - \frac{C(t)\big|_{z=-E}}{E(t)} \frac{d(-E(t))}{dt} \tag{A1}$$

where the overbar notation indicates the vertical average of a quantity from the depth of the bottom of the euphotic zone (computed daily as the 0.1% light level; $-E(t)$) to the surface. The quantities F_C and B_C denote the physical and biological processes, respectively, which affect the concentration of component C, and the final term of Eq. (A1) arises via the Liebniz rule, since the lower integral limit ($E(t)$) is a function of time (see FH01, Eq. (2)). The vertical profiles of P, Z, A, N and D are specified, based on observations from the JGOFS EqPac experiment (see FH01, Fig. 6).

The physical processes (advection and sinking) affecting the concentrations of each of the model components, can be written mathematically as:

$$\overline{F_P} = -\frac{1}{E(t)} \int_{-E(t)}^{0} w \frac{\partial P}{\partial z}\, dz \tag{A2}$$

$$\overline{F_Z} = -\frac{1}{E(t)} \int_{-E(t)}^{0} (w + w_Z) \frac{\partial Z}{\partial z}\, dz \tag{A3}$$

$$\overline{F_N} = -\frac{1}{E(t)} \int_{-E(t)}^{0} \left(u \frac{\partial N}{\partial x} + v \frac{\partial N}{\partial y} + w \frac{\partial N}{\partial z} \right) dz \tag{A4}$$

$$\overline{F_A} = -\frac{1}{E(t)} \int_{-E(t)}^{0} w \frac{\partial A}{\partial z}\, dz \tag{A5}$$

$$\overline{F_D} = -\frac{1}{E(t)}\int_{-E(t)}^{0}(w + w_D)\frac{\partial D}{\partial z}\,dz \tag{A6}$$

where w_Z and w_D represent the sinking rates of zooplankton and detritus, respectively. The various biological pathways for nitrogen cycling in the model ecosystem (Fig. 1) are described by the following equations:

$$\overline{B_P} = \overline{PP}(Fe, I, \bar{P}) - \bar{G}(\bar{P}, \bar{Z}) - \varphi_P\bar{P} \tag{A7}$$

$$\overline{B_Z} = \gamma\bar{G}(\bar{P}, \bar{Z}) - \varphi_Z\bar{Z} \tag{A8}$$

$$\overline{B_N} = -\overline{NP}(Fe, I, \bar{P}, \bar{A}) \tag{A9}$$

$$\overline{B_A} = -\overline{RP}(Fe, I, \bar{P}, \bar{A}) + \beta\varphi_Z\bar{Z} + r_D\bar{D} \tag{A10}$$

$$\overline{B_D} = \varphi_P\bar{P} + (1 - \beta)\varphi_Z\bar{Z} + (1 - \gamma)\bar{G}(\bar{P}, \bar{Z}) - r_D\bar{D} \tag{A11}$$

where the values and definitions of specific parameters are given in Table 1. A brief overview of these various processes will now be given, but the reader is referred to FH01 for a more thorough discussion of the model formulations.

The biological processes affecting phytoplankton biomass include natural mortality ($\varphi_P\bar{P}$), grazing by zooplankton ($\bar{G}$):

$$\bar{G}(\bar{P}, \bar{Z}) = g\bar{P}\bar{Z}\Lambda(1 - e^{-\bar{P}\Lambda}) \tag{A12}$$

and primary production ($\overline{PP}$). Because recent results of *in situ* iron additions to macronutrient-rich equatorial waters during the IronEx cruises have unequivocally established that the availability of iron limits the cell division rates and abundance of phytoplankton (Frost, 1996; Behrenfeld *et al.,* 1996), iron limitation is assumed *a priori.* Thus, instead of *re-testing* the iron hypothesis, the novel approach of *assuming* iron limitation and examining the implications for marine ecosystem structure at 0N, 140W is taken. Until more information becomes available on iron chemistry and the specific roles various forms of iron play in equatorial ecosystems, an explicit iron model is not justified. Therefore, in this study iron concentration is not included as a separate model component, but rather it is included in the growth term where iron limitation is specified. Primary production is modeled as:

$$\overline{PP} = \frac{1}{E}\int_{-E}^{0}\frac{Fe(z)}{Fe(z) + k_{Fe}}P(z)\int_{0}^{1}P_{mx}(1 - e^{-I\alpha/P_{mx}})d\tau dz \tag{A13}$$

where $P_{mx}(\tau) = P_M \sin(2\pi(\tau - 0.25))$ for $0.25 < \tau < 0.75$, and $P_{mx}(\tau) = 0$ otherwise, and the photosynthetically active portion of the visible light spectrum (PAR) is computed as:

$$I(\tau, z) = \begin{cases} 0 & \text{for } \tau < 0.25 \text{ or } \tau > 0.75 \\ I_0(1 - C_s)\sin(2\pi(\tau - 0.25))R(z) & \text{for } 0.25 < \tau < 0.75. \end{cases}$$

In these formulations, τ represents nondimensionalized time ($\tau = t/24$ h, where $t = [0, 24\text{ h}]$), I_0 is the clear sky value of PAR, C_s is fraction cloud cover, and $R(z)$ is the depth dependent attenuation as described in Appendix B of FH01. Iron concentration ($Fe(z)$) is determined from a bilinear approximation to the empirical formulation of Gordon *et al.* (1997): $Fe(z) = \text{MAX}[Fe_{min}, Fe|_{z=-100} - m_{Fe}(z + 100)]$, where iron concentrations at 100 m depth ($Fe|_{z=-100}$) are computed from a $Fe{:}T$ regression.

A fraction (γ) of the grazed phytoplankton is assumed to represent zooplankton growth from assimilated ingestion, and is partially offset by a generalized loss term ($\varphi_Z \bar{Z}$). A fraction (β) of this loss term is attributed to zooplankton excretion, and the remainder represents losses such as natural mortality and predation. Primary production is supported by both nitrate uptake (new production; $\overline{NP}$) and ammonium uptake (regenerated production; $\overline{RP}$). Recently a strong suppressing effect of ammonium on nitrate uptake rates has been observed in the central equatorial Pacific (McCarthy *et al.,* 1996). Therefore, if ammonium concentrations are high enough to provide enough nitrogen to fuel all primary production, then $\overline{RP} = \overline{PP}$. Otherwise,

$$\overline{RP} = \mu_{mx} \frac{A}{k_A + A} \bar{P}. \tag{A14}$$

where μ_{mx} is the iron-saturated growth rate. New production ($\overline{NP}$) is defined as that portion of total primary production that is supported by nitrate uptake, instead of by ammonium utilization, i.e. $\overline{NP} = \overline{PP} - \overline{RP}$.

Other biological processes affecting the ammonium balance include zooplankton excretion and recycling via the detrital pool ($r_D \bar{D}$), where r_D represents a generalized rate at which detritus is recycled into ammonium. Biological processes affecting the detrital pool include contributions from phytoplankton and zooplankton mortality, unassimilated grazing, and the loss of detrital nitrogen to ammonium nitrogen via recycling.

REFERENCES

Abbott, M. R. 1992. Workshop on modeling and satellite data assimilation. U.S. JGOFS Planning Report Number 14, WHOI, Woods Hole, MA.

Aikman, F., G. L. Mellor, T. Ezer, D. Sheinin, P. Chen, L. Breaker and D. B. Rao. 1996. Towards an operational nowcast/forecast system for the U.S. East Coast, *in* Modern Approaches to Data Assimilation in Ocean Modeling, P. Malanotte-Rizzoli, ed., Elsevier Oceanography Series, *61,* Amsterdam, The Netherlands, 347–376.

Armstrong, R. A., J. L. Sarmiento and R. D. Slater. 1995. Monitoring ocean productivity by assimilating satellite chlorophyll into ecosystem models, *in* Ecological Time Series, T. Powell and J. Steele, eds., Chapman and Hall, NY, 371–390.

Barth, N. and C. Wunsch. 1990. Oceanographic experiment design by simulated annealing. J. Phys. Oceanogr., *20,* 1249–1263.

Behrenfeld, M. J., A. J. Bale, Z. S. Kolber, J. Aiken and P. G. Falkowski. 1996. Confirmation of iron limitation of phytoplankton photosynthesis in the equatorial Pacific Ocean. Nature, *383,* 508–511.

Bennett, A. F. 1992. Inverse Methods in Physical Oceanography, Cambridge Univ. Press, NY, 346 pp.

Carnes, M. R., D. N. Fox, R. C. Rhodes and O. M. Smedstad. 1996. Data assimilation in a North Pacific Ocean monitoring and prediction system, *in* Modern Approaches to Data Assimilation in Ocean Modeling, P. Malanotte-Rizzoli, ed., Elsevier Oceanography Series, *61,* Amsterdam, The Netherlands, 319–346.

DeMaria, M. and R. W. Jones. 1993. Optimization of a hurricane track forecast model with the adjoint model equations. Mon. Weather Rev., *121,* 1730–1745.

Evans, G. T. 1999. The role of local models and data sets in the Joint Global Ocean Flux Study. Deep-Sea Res. I, *46,* 1369–1389.

Evensen, G. 1992. Using the extended Kalman filter with a multilayer quasi-geostrophic ocean model. J. Geophys. Res., *97,* 17,905–17,924.

Fasham, M., H. W. Ducklow and S. M. McKelvie. 1990. A nitrogen-based model of plankton dynamics in the oceanic mixed layer. J. Mar. Res., *48,* 591–639.

Fasham, M. and G. T. Evans. 1995. The use of optimization techniques to model marine ecosystem dynamics at the JGOFS station at 47°N 20°W. Phil. Trans. Royal Soc. London B, *348,* 203–209.

Fasham, M. J. R., J. L. Sarmiento, R. D. Slater, H. W. Ducklow and R. Williams. 1993. Ecosystem behavior at Bermuda Station "S" and Ocean Weather Station "India": a general circulation model and observational analysis. Global Biogeochem. Cycles, *7,* 379–415.

Friedrichs, M. A. M. 1999. Physical control of biological processes in the central equatorial Pacific: A data assimilative modeling study. Ph.D. Thesis, Old Dominion University, Norfolk, VA, 195 pp.

——— 2001. Assimilation of JGOFS EqPac and SeaWiFS data into a marine ecosystem model of the central equatorial Pacific Ocean. Deep-Sea Res. II, *49,* 289–319.

Friedrichs, M. A. M. and E. E. Hofmann. 2001. Physical control of biological processes in the central equatorial Pacific. Deep-Sea Res. I, *48,* 1023–1069.

Frost, B. W. 1996. Phytoplankton bloom on iron rations. Nature, *383,* 475–476.

Ghil M. and P. Malanotte-Rizzoli. 1991. Data assimilation in meteorology and oceanography. Adv. Geophys., *33,* 151–266.

Gilbert, J. C. and C. Lemarechal. 1989. Some numerical experiments with variable-storage quasi-newton algorithms. Math. Program., *45,* 405–435.

Gordon, R. M., K. H. Coale and K. S. Johnson. 1997. Iron distributions in the equatorial Pacific: Implications for new production. Limnol. Oceanogr., *42,* 419–431.

Gunson, J. R. and P. Malanotte-Rizzoli. 1996a. Assimilation studies of open-ocean flows, 1, Estimation of initial and boundary conditions. J. Geophys. Res., *101,* 28457–28472.

——— 1996b. Assimilation studies of open-ocean flows, 2, Error measures with strongly nonlinear dynamics. J. Geophys. Res., *101,* 28473–28488.

Gunson, J. R., A. Oschlies and V. Garcon. 1999. Sensitivity of ecosystem parameters to simulated satellite ocean color data using a coupled physical-biological model of the North Atlantic. J. Mar. Res., *57,* 613–639.

Harmon, R. and P. Challenor. 1997. A Markov Chain Monte Carlo method for estimation and assimilation into models. Ecol. Model., *101,* 41–59.

Hofmann, E. E. and M. A. M. Friedrichs. 2001a. Predictive modeling for marine ecosystem models, *in* The Sea: Volume 12: Biological-Physical Interactions in the Ocean, A. R. Robinson, J. R. McCarthy and B. J. Rothschild, eds., John Wiley & Sons, 640 pp.

——— 2001b. Models: biogeochemical data assimilation, *in* Encyclopedia of Ocean Sciences, Vol. 1, M. J. R. Fasham, J. H. Steele, S. Thorpe and K. Turekian, eds., Academic Press, London, 302–308.

Holland, W. R. and A. D. Hirschman. 1972. A numerical calculation of the circulation in the North Atlantic Ocean. J. Phys. Oceanogr., *2,* 336–354.

Holland, W. R. and P. Malanotte-Rizzoli. 1989. Assimilation of altimeter data into an ocean circulation model: space versus time resolution studies. J. Phys. Oceanogr., *19,* 1507–1534.

Hurtt, G. C. and R. A. Armstrong. 1996. A pelagic ecosystem model calibrated with BATS data. Deep-Sea Res. II, *43,* 625–651.

——— 1999. A pelagic ecosystem model calibrated with BATS and OWS I data. Deep-Sea Res. I, *46,* 27–61.

Ishizaka, J. 1990. Coupling of Coastal Zone Color Scanner data to a physical-biological model of the southeastern U.S. continental shelf ecosystem 3. Nutrient and phytoplankton fluxes and CZCS data assimilation. J. Geophys. Res., *95,* 20201–20212.

Kruger, J. 1993. Simulated annealing: a tool for data assimilation into an almost steady model state. J. Phys. Oceanogr., *23,* 679–688.

Landry, M. R., J. Constantinou and J. Kirshtein. 1995. Microzooplankton grazing in the central equatorial Pacific during February and August, 1992. Deep-Sea Res. II, *42,* 657–671.

Lardner, R. W. and S. K. Das. 1994. Optimal estimation of eddy viscosity for a quasi-three-dimensional numerical tidal and storm surge model. Int. J. Numer. Methods Fluids, *18,* 295–312.

Lawson, L. M., Y. H. Spitz, E. E. Hofmann and R. B. Long. 1995. A data assimilation technique applied to a predator-prey model. Bull. Math. Biol., *57,* 593–617.

Lawson, L. M., E. E. Hofmann and Y. H. Spitz. 1996. Time series sampling and data assimilation in a simple marine ecosystem model. Deep-Sea Res. II, *43,* 625–651.

Leonard, C. L., C. R. McClain, R. Murtugudde, E. E. Hofmann and L. W. Harding. 1999. An iron-based ecosystem model of the central equatorial Pacific. J. Geophys. Res., *104,* 1325–1341.

Malanotte-Rizzoli, P. and E. Tziperman. 1996. The oceanographic data assimilation problem: overview, motivation and purposes, *in* Modern Approaches to Data Assimilation in Ocean Modeling, P. Malanotte-Rizzoli, ed., Elsevier Oceanography Series, *61,* Amsterdam, The Netherlands, 3–17.

Malanotte-Rizzoli, P. and R. E. Young. 1995. Assimilation of global versus local data sets into a regional model of the Gulf Stream system 1. Data effectiveness. J. Geophys. Res., *100,* 24773–24796.

Matear, R. J. 1995. Parameter optimization and analysis of ecosystem models using simulated annealing: A case study at Station P. J. Mar. Res., *53,* 571–607.

McCarthy, J. J., C. Garside, J. L. Nevins and R. T. Barber. 1996. New production along 140°W in the equatorial Pacific during and following the 1992 El Niño event. Deep-Sea Res. II, *43,* 1065–1093.

McClain, C. R., J. L. Cleave, G. C. Feldman, W. W. Gregg, S. B. Hooker and N. Kuring. 1998. Science quality SeaWiFS data for global biosphere research. Sea Tech., *39,* 10–15.

McClain, C. R., R. Murtugudde and S. Signorini. 1999. A simulation of biological processes in the equatorial Pacific warm pool at 165°E. J. Geophys. Res., *104,* 18305–18322.

McGillicuddy, D. J., D. R. Lynch, A. M. Moore, W. C. Gentleman, C. S. Davis and C. J. Meise. 1998. An adjoint data assimilation approach to diagnosis of physical and biological controls on *Pseudocalanus* spp. in the Gulf of Maine-Georges Bank Region. Fisheries Oceanogr., *7,* 205–218.

McPhaden, M. J., A. J. Busalacchi, R. Cheney, J.-R. Donguy, K. S. Gage, D. Halpern, M. Ji, P. Julian, G. Meyers, G. T. Mitchum, P. P. Niiler, J. Picaut, R. W. Reynolds, N. Smith and K. Takeuchi. 1998. The Tropical Ocean Global Atmosphere (TOGA) observing system: A decade of progress. J. Geophys. Res., *103,* 14169–14240.

Moisan, J. R. and E. E. Hofmann. 1996. Modeling nutrient and plankton processes in the California coastal transition zone. 2. A three-dimensional physical-bio-optical model. J. Geophys. Res., *101,* 22,677–22,691.

Murray, J. W., R. T. Barber, M. R. Roman, M. P. Bacon and R. A. Feely. 1994. Physical and biological controls on carbon cycling in the equatorial Pacific. Science, *266,* 58–65.

Murray, J. W., E. Johnson and C. Garside. 1995. A U.S. JGOFS process study in the equatorial Pacific (EqPac): Introduction. Deep-Sea Res. II, *42,* 275–293.

Najjar, R. G., J. L. Sarmiento and J. R. Toggweiler. 1992. Downward transport and fate of organic matter in the ocean: Simulations with a general circulation model. Global Biogeochem. Cycles, *6,* 45–76.

Peloquin, R. A. 1992. The navy ocean modeling and prediction program. Oceanography, *1,* 4–8.

Prunet, P., J. F. Minster, V. Echevin and I. Dadou. 1996a. Assimilation of surface data in a one-dimensional physical-biogeochemical model of the surface ocean 2. adjusting a simple trophic model to chlorophyll, temperature, nitrate, and pCO_2 data. Global Biogeochem. Cycles, *10,* 139–158.

Prunet, P., J. F. Minster, D. Ruiz-Pino and I. Dadou. 1996b. Assimilation of surface data in a one-dimensional physical-biogeochemical model of the surface ocean 1. method and preliminary results. Global Biogeochem. Cycles, *10,* 111–138.

Sarmiento, J. L. and R. A. Armstrong. 1997. U.S. JGOFS Synthesis and Modeling Project Implementation Plan: The role of Oceanic Processes in the Global Carbon Cycle, U.S. JGOFS Planning and Coordination Office, WHOI, Woods Hole, MA.

Sarmiento, J. L. and K. Bryan. 1982. An ocean transport model for the North Atlantic. J. Geophys. Res., *87,* 394–408.

Sarmiento, J., B. Frost and J. Wroblewski. 1987. Modeling in GOFS, U.S. GOFS Planning Report Number 4, WHOI, Woods Hole, MA.

Seiler, U. 1993. Estimation of open boundary conditions with the adjoint method. J. Geophys. Res., *98,* 22855–22870.

Semovski, S. V. and B. Wozniak. 1995. Model of the annual phytoplankton cycle in the marine ecosystem: assimilation of monthly satellite chlorophyll data for the N. Atlantic and Baltic. Oceanologia, *37,* 3–31.

Sheinbaum, J. 1995. Variational assimilation of simulated acoustic tomography data and point observations: A comparative study. J. Geophys. Res., *100,* 20745–20761.

Spitz, Y. H., J. R. Moisan, M. R. Abbott and J. G. Richman. 1998. Data assimilation and a pelagic ecosystem model: parameterization using time series observations. J. Mar. Syst., *16,* 51–68.

Tziperman, E. and W. C. Thacker. 1989. An optimal-control/adjoint-equations approach to studying the oceanic general circulation. J. Phys. Oceanogr., *19,* 1471–1485.

Ullman, D. S. and R. E. Wilson. 1998. Model parameter estimation from data assimilation modeling: temporal and spatial variability of the bottom drag coefficient. J. Geophys. Res., *103,* 5531–5549.

Vallino, J. J. 2000. Improving marine ecosystem models: Use of data assimilation and mesocosm experiments. J. Mar. Res., *58,* 117–164.

Verity, P. G., D. K. Stoecker, M. E. Sieracki and J. R. Nelson. 1996. Microzooplankton grazing of primary production in the equatorial Pacific. Deep-Sea Res. II, *43,* 1227–1256.

Wunsch, C. 1996. The Ocean Circulation Inverse Problem. Cambridge Univ. Press, NY, 442 pp.

Wunsch, C. and A. E. Gill. 1976. Observations of equatorially trapped waves in Pacific sea level variations. Deep-Sea Res., *23,* 371–390.

Received: *17 June, 2001;* revised: *25 September, 2001.*